

POLITECNICO DI TORINO

*Department of Mechanical & Aerospace engineering*

MASTERS THESIS

---

**Multi-objective Optimal control strategy  
for Ultra-Low NO<sub>x</sub> compliance in  
Heavy-Duty diesel engines**

---



**Politecnico  
di Torino**



*Author:*

**Pradyumna Saripalli**  
DIMEAS, Politecnico di  
Torino

*Supervisor:*

**Dr. Yongsoon Yoon**  
Department of Mechanical  
Engineering, Oakland University  
**Dr. Daniela Misul**  
DIMEAS, Politecnico di Torino

*A thesis submitted in fulfillment of requirements for the degree of Master of  
Science in Automotive engineering.*

November 16, 2022



# Declaration of Authorship

I, Pradyumna Saripalli , declare that this thesis titled, “Multi-objective Optimal control strategy for Ultra-Low NOx compliance in Heavy-Duty diesel engines” and the work presented in it are my own. I confirm that:

- This work was done wholly or mainly while in candidature for a research degree at the **Politecnico di Torino**.
- Where any part of this thesis has previously been submitted for a degree or any other qualification at this University or any other institution, this has been clearly stated.
- Where I have consulted the published work of others, this is always clearly attributed.
- Where I have quoted from the work of others, the source is always given. With the exception of such quotations, this thesis is entirely my own work.
- I have acknowledged all main sources of help.
- Where the thesis is based on work done by myself jointly with others, I have made clear exactly what was done by others and what I have contributed myself.

Signature:



Date:

16/11/2022



# Abstract

Pradyumna Saripalli

*Multi-objective Optimal control strategy for Ultra-Low NO<sub>x</sub> compliance in Heavy-Duty diesel engines*

The ultra-low nitrogen oxides (NO<sub>x</sub>) regulation, recently proposed by California Air Resource Board, will require a 90 % reduction in tailpipe NO<sub>x</sub> emission from the current standards implemented in 2010 without increasing greenhouse gas emissions. Such a strong drive toward clean mobility in the heavy-duty sector has led to significant research in aggressive thermal management, advanced control systems like cylinder deactivation, and improving catalytic converters and electrification, demanding additional hardware development and increasing cost. For compliance with this stringent regulation, it is essential to achieve low engine-out NO<sub>x</sub> and fast catalyst light-off simultaneously during cold start and low-load conditions. However, due to a tradeoff between these two requirements, conventional pseudo-logic-based control methods have shown limited performance even with significant calibration effort. This research work aims at developing a model-based optimal control strategy for a high-level combustion controller of heavy-duty diesel engines during low-load transient operating conditions. Toward this end, a control-oriented combustion model is developed. Then, a multi-objective optimization problem is formulated to find optimal high-level control commands, including fuel flow rate, charge flow rate, intake oxygen concentration and the start of injection, to be achieved by low-level controllers. The globally optimal solution to the proposed control problem is obtained offline using dynamic programming. Numerical studies carried out in this work demonstrate that the proposed method can deal with conflicting requirements in an effective way. This method also has the potential to give insight into calibrations of diesel engine control maps.

Keywords: Control-oriented combustion models, Optimal control, Dynamic programming, Heavy-Duty diesel engines, Ultra-Low NO<sub>x</sub> emissions.



# Acknowledgements

The presented work in this report is the summary of scientific research carried out to fulfil the requirements of the M.Sc course at the Politecnico di Torino (PoliTO). This research work was carried out at Oakland University (OU), Michigan, under a joint mobility program between Politecnico di Torino and Oakland University. The author wishes to thank Dr Brian Sangeorzan and Dr Yongsoon Yoon from OU for providing the opportunity to work on this project.

The author expresses his sincere gratitude to his supervisor Dr Yoon for his valuable advice and guidance throughout this work. The author would also like to thank his advisor from PoliTO, Dr Daniela Misul, for her continuous support and feedback on the final report. The author is indebted to Prof. Giovanni Belingardi and Prof. Maria Piu Cavatorta at PoliTo for considering him to be a part of the international thesis mobility program.

Lastly, but most importantly, the author is indebted to his family and friends for their never-ending love and support...



# Contents

<b>Declaration of Authorship</b>	<b>iii</b>
<b>Abstract</b>	<b>v</b>
<b>Contents</b>	<b>ix</b>
<b>List of Figures</b>	<b>xi</b>
<b>List of Tables</b>	<b>xiii</b>
<b>List of Abbreviations</b>	<b>xv</b>
<b>List of Symbols</b>	<b>xvii</b>
<b>1 Introduction</b>	<b>1</b>
1.1 Phases of diesel combustion	1
1.2 Diesel engine emissions	2
1.3 NO <sub>x</sub> formation	2
1.4 Legislation	4
1.5 NO <sub>x</sub> control techniques	4
1.5.1 In-cylinder NO <sub>x</sub> control techniques	5
Air Fuel ratio	5
Boost	6
Injection timing	6
Exhaust gas recirculation	7
1.5.2 After-treatment systems (NO <sub>x</sub> )	8
Ammonia SCR catalysts	8
DeNO <sub>x</sub> catalysts	9
Lean NO <sub>x</sub> trap	9
1.5.3 Engine thermal management	10
Cylinder deactivation	10
Air cooler and turbine bypass	10
1.6 Challenges in NO <sub>x</sub> control	11
1.7 Scope of this work	12
<b>2 Diesel engine simulation model</b>	<b>15</b>
2.1 Resizing engine and performance maps	15
2.2 Design of experiments	17
2.2.1 Latin Hypercube sampling	17
2.2.2 Sampling Engine Operational Points	17

2.3	Engine performance plots . . . . .	20
<b>3</b>	<b>Control oriented model</b>	<b>21</b>
3.1	Background . . . . .	21
3.1.1	Phenomenological Models . . . . .	21
3.1.2	Empirical Models . . . . .	21
3.1.3	Semi-Empirical Models . . . . .	21
3.2	Multi Layer Perceptron Neural Networks . . . . .	22
3.3	Multi-Variable Polynomial Regression . . . . .	23
3.4	Control-Oriented HD Diesel engine Model . . . . .	24
3.4.1	Neural Network model . . . . .	24
	Network Architecture . . . . .	24
	Training . . . . .	24
	Model Performance . . . . .	25
3.4.2	Polynomial model . . . . .	28
	Model details . . . . .	29
	Model Performance . . . . .	30
<b>4</b>	<b>Global Optimisation</b>	<b>31</b>
4.1	Background . . . . .	31
4.1.1	Working principle . . . . .	31
4.1.2	DP Limitations . . . . .	32
4.2	Problem formulation . . . . .	33
4.2.1	Discrete HD Engine model . . . . .	33
4.2.2	Optimal Combustion Control Design . . . . .	34
4.3	DP Simulation results . . . . .	35
4.3.1	Sensitivity analysis . . . . .	35
4.3.2	Single-Objective Limit Case Studies . . . . .	36
4.3.3	Multi-Objective Optimization . . . . .	41
<b>5</b>	<b>Scope for future work</b>	<b>43</b>
5.1	Reinforcement Learning Background . . . . .	43
5.1.1	Elements of Reinforcement Learning . . . . .	43
5.1.2	RL framework . . . . .	44
5.2	RL based combustion controller . . . . .	44
5.2.1	RL environment . . . . .	45
5.2.2	Reward function . . . . .	45
5.2.3	Actions . . . . .	45
5.3	Summary . . . . .	45
<b>6</b>	<b>Conclusion</b>	<b>47</b>
	<b>Bibliography</b>	<b>49</b>

# List of Figures

1.1	Different phases of diesel combustion process. . . . .	1
1.2	Pollutant formation during pre-mixed and mixing-controlled phases of diesel combustion. . . . .	3
1.3	HD-FTP transient drive cycle . . . . .	5
1.4	Effect of equivalence ratio on NO <sub>x</sub> formation. . . . .	6
1.5	Effect of injection timing on brake specific NO <sub>x</sub> emissions and fuel consumption. . . . .	7
1.6	Effect of EGR on brake specific specific NO <sub>x</sub> and soot emissions . . . . .	7
1.7	Working principle schematic of an SCR system. . . . .	8
1.8	Operating mechanism of a Lean NO <sub>x</sub> trap system. . . . .	9
1.9	Various technologies for achieving Ultra-Low NO <sub>x</sub> emissions [5]. . . . .	10
1.10	Cylinder deactivation technology. . . . .	11
1.11	Map-based HD diesel engine simulation: exhaust gas temperature during low and medium load operation. . . . .	12
1.12	HD diesel engine configuration: high-pressure EGR, variable geometry turbocharger, after-treatment system (SCR). . . . .	13
1.13	Controller hierarchy representation of a diesel engine. . . . .	14
2.1	Mathworks CI engine dynamometer reference application. . . . .	16
2.2	Rescaled engine specification for a 6.7 litre diesel engine. . . . .	16
2.3	Unique samples of Fuel mass & RPM obtained using LHS DoE generator. . . . .	18
2.4	Engine simulation model and layout. . . . .	19
2.5	Steady state DoE performance plots . . . . .	20
3.1	Feed-forward type neural networks with fully connected nodes [19]. . . . .	22
3.2	Representation of network computations in a neural network [19]. . . . .	23
3.3	Neural network model of HD Diesel Engine. . . . .	24
3.4	Sensitivity analysis of NN Model prediction as a function of hidden layer nodes. . . . .	25
3.5	NN Model dynamic performance matrix. . . . .	26
3.6	Neural Network model Regression plots . . . . .	27
3.7	Neural network model dynamic performance plots . . . . .	28
3.8	Polynomial model training flow chart. . . . .	29
3.9	Polynomial model training flow chart. . . . .	30
4.1	Dynamic Programming algorithm: study of the possible patterns (left); selection of the pattern related to minimum fuel consumption (right) [25]. . . . .	32
4.2	Engine out NO <sub>x</sub> emissions as a function of state variable grid resolution. . . . .	36
4.3	Computation time for various optimisation iterations. . . . .	37
4.4	Optimal control sequence for different single-objective optimisation strategies. . . . .	38

4.5	Normalized optimal control sequence for three different strategies during idle, part load and full load conditions. Note that positive SOI means before-top-dead-center in this figure. . . . .	40
4.6	Performance comparison among different strategies. . . . .	42
5.1	The agent-environment interaction in an RL framework. . . . .	44
5.2	Simulink block diagram of HD Diesel engine model within RL framework. . . . .	44

## List of Tables

2.1	Reference engine details . . . . .	15
2.2	DoE variable operating ranges . . . . .	18
4.1	Control factor levels and total combinations corresponding to various iterations.	35
4.2	Three operational conditions . . . . .	39
4.3	Weighting parameters . . . . .	41



# List of Abbreviations

<b>HD</b>	<b>Heavy Duty</b>
<b>RPM</b>	<b>Revolutions per minute</b>
<b>CI</b>	<b>Compression Ignition</b>
<b>SOC</b>	<b>Start of Combustion</b>
<b>SOI</b>	<b>Start of Injection</b>
<b>BMEP</b>	<b>Brake mean effective pressure</b>
<b>NOx</b>	<b>Nitrogen Oxides</b>
<b>FTP</b>	<b>Federal Test Procedure</b>
<b>NYNF</b>	<b>New York Non Freeway</b>
<b>LANF</b>	<b>Los Angeles Non Freeway</b>
<b>LAFY</b>	<b>Los Angeles Freeway</b>
<b>EPA</b>	<b>Environment Protection Agency</b>
<b>EGR</b>	<b>Exhaust Gas Recirculation</b>
<b>SCR</b>	<b>Selective Catalytic Reduction</b>
<b>DEF</b>	<b>Diesel Exhaust Fluid</b>
<b>LNT</b>	<b>Lean NOx Trap</b>
<b>CDA</b>	<b>Cylinder Deactivation</b>
<b>VGT</b>	<b>Variable Geometry Turbine</b>
<b>DOE</b>	<b>Design of Experiments</b>
<b>LHS</b>	<b>Latin Hypercube Sampling</b>
<b>ANN</b>	<b>Artificial Neural Networks</b>
<b>MIMO</b>	<b>Multiple Input Multiple Output</b>
<b>DP</b>	<b>Dynamic Programming</b>
<b>MLP</b>	<b>Multi Layer Perceptron</b>
<b>MSE</b>	<b>Mean Squared Error</b>
<b>RL</b>	<b>Reinforcement Learning</b>
<b>DDPG</b>	<b>Deep Deterministic Policy Gradient</b>



# List of Symbols

$T_e$	Engine Torque	Nm
$N_e$	Engine speed	$\text{rads}^{-1}$
$T_c$	Coolant temperature	K
$F_i$	Fuel mass per injection	mg
$P_f$	Fuel pressure	bar
$m_a$	Intake air flow rate	$\text{kg s}^{-1}$
$m_f$	Fuel flow rate	$\text{kg s}^{-1}$
$m_c$	Charge flow rate	$\text{kg s}^{-1}$
$X_{O_2}$	Oxygen concentration	%
$\theta_{soi}$	Start of Injection timing	deg CA
$m_{exh}$	Exhaust flow rate	$\text{kg s}^{-1}$
$Y_i$	Pollutant mass fractions	[-]
$m_{NOx}$	NOx flow rate	$\text{kg s}^{-1}$
$m_f^a$	Actual Fuel flow rate	$\text{kg s}^{-1}$
$m_f^d$	Desired Fuel flow rate	$\text{kg s}^{-1}$
$m_c^a$	Actual Charge flow rate	$\text{kg s}^{-1}$
$m_c^d$	Desired Charge flow rate	$\text{kg s}^{-1}$
$X_{O_2}^a$	Actual Oxygen concentration	%
$X_{O_2}^d$	Desired Oxygen concentration	%
$e_{exh}$	Exhaust specific enthalpy	$\text{kJ kg}^{-1}$
$E_{exh}$	Exhaust enrrgy	$\text{kJ s}^{-1}$
$\bar{m}_{NOx}$	Brake specific NOx emission	$\text{kg}/(\text{kWh})$
$\bar{m}_f$	Brake specific fuel consumption	$\text{kg}/(\text{kWh})$
$\theta_{soi}^a$	Actual Start of Injection timing	deg CA
$\theta_{soi}^d$	Desired Start of Injection timing	deg CA



# Chapter 1

## Introduction

Diesel engines find wide usage in heavy-duty (HD) applications due to higher efficiencies and higher torque delivery at low engine speeds. Due to the high reactivity of diesel fuel, the fuel is sprayed directly into the combustion chamber instead of mixing with air and then inducting into the engine. Hence, the engines operating on diesel fuel are referred to as Compression Ignition (CI) engines. In CI engines, the fuel-injection system directly injects diesel fuel inside the combustion chamber at high pressure, just before the desired Start of Combustion (SOC) timing. The fuel atomizes into a spray because of the high injection pressures and mixes with the turbulent air. The highly-reactive diesel spray reaches its self-ignition temperature and burns while interacting with the hot compressed air, thus generating power.

### 1.1 Phases of diesel combustion

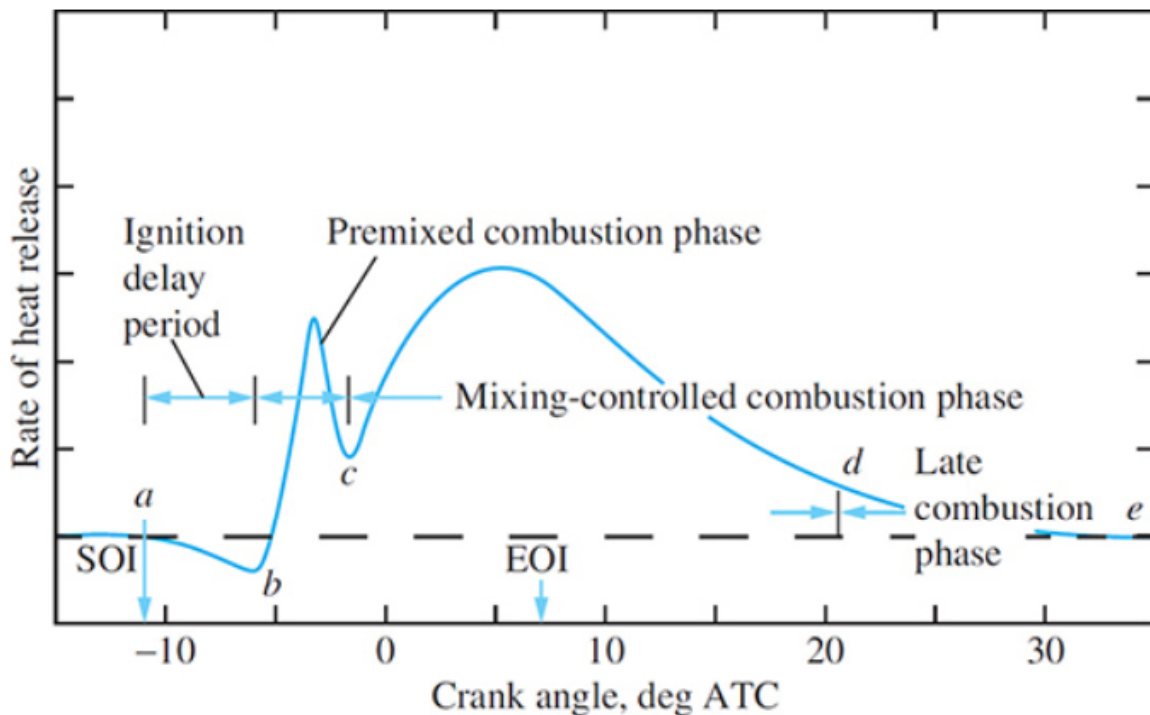


FIGURE 1.1: Different phases of diesel combustion process.

The burning of diesel fuel takes place in four different phases, as represented in Fig. 1.1 [1].

The Ignition delay ( $ab$ ) is the time elapsed between the Start of Injection (SOI) and SOC, and is because of the fuel atomization, vaporisation and initial chemical reactions during mixing.

During the pre-mixed burning phase ( $bc$ ), the fuel accumulated in the combustion chamber during Ignition delay heats up and burns almost instantaneously, resulting in high heat energy release.

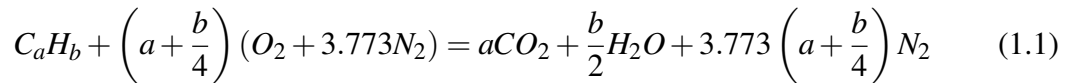
After the initial heat release, as the burning rate is governed by further mixing of fuel & air ( $cd$ ). Though several processes - fuel atomization, vaporisation and mixing are involved during this phase, burning rate is primarily governed by fuel- air mixing.

Finally, the late combustion phase ( $de$ ) takes places during early expansion stroke and because various reasons- residual unburned fuel, fractions of energy rich elements in soot and release of fuel rich combustion products.

As majority of the heat release takes place during pre-mixed combustion and mixed-controlled combustion phases, the in-cylinder temperatures as high and thus aid Nitrogen oxides ( $NO_x$ ) formation.

## 1.2 Diesel engine emissions

Under ideal operating conditions, hydrocarbon-based fuel combustion should lead to non-toxic combustion bi-products-  $CO_2$ ,  $H_2O$  and  $N_2$ , as represented in eqn. 1.1.



However, this is seldom the case in real-world operations, and the engine operation results in harmful pollutant emissions in the form of unburned hydrocarbons ( $HC$ ), carbon monoxide ( $CO$ ), particulate matter ( $PM$ ) and Nitrogen oxides ( $NO_x$ ), as represented in Fig. 1.2 [1].

## 1.3 NO<sub>x</sub> formation

In diesel engines,  $NO_x$  emissions are usually 70-90% comprised of Nitrogen oxide ( $NO$ ), and 30-10% Nitrogen dioxide ( $NO_2$ ).  $NO$  is formed as a by-product of the combustion process due to oxidation of atmospheric  $N_2$  under high temperature. The  $NO_x$  formation mechanism in internal combustion engines is a thermal mechanism known as the extended Zeldovich mechanism, represented by Eqns. (1.2) - (1.4).



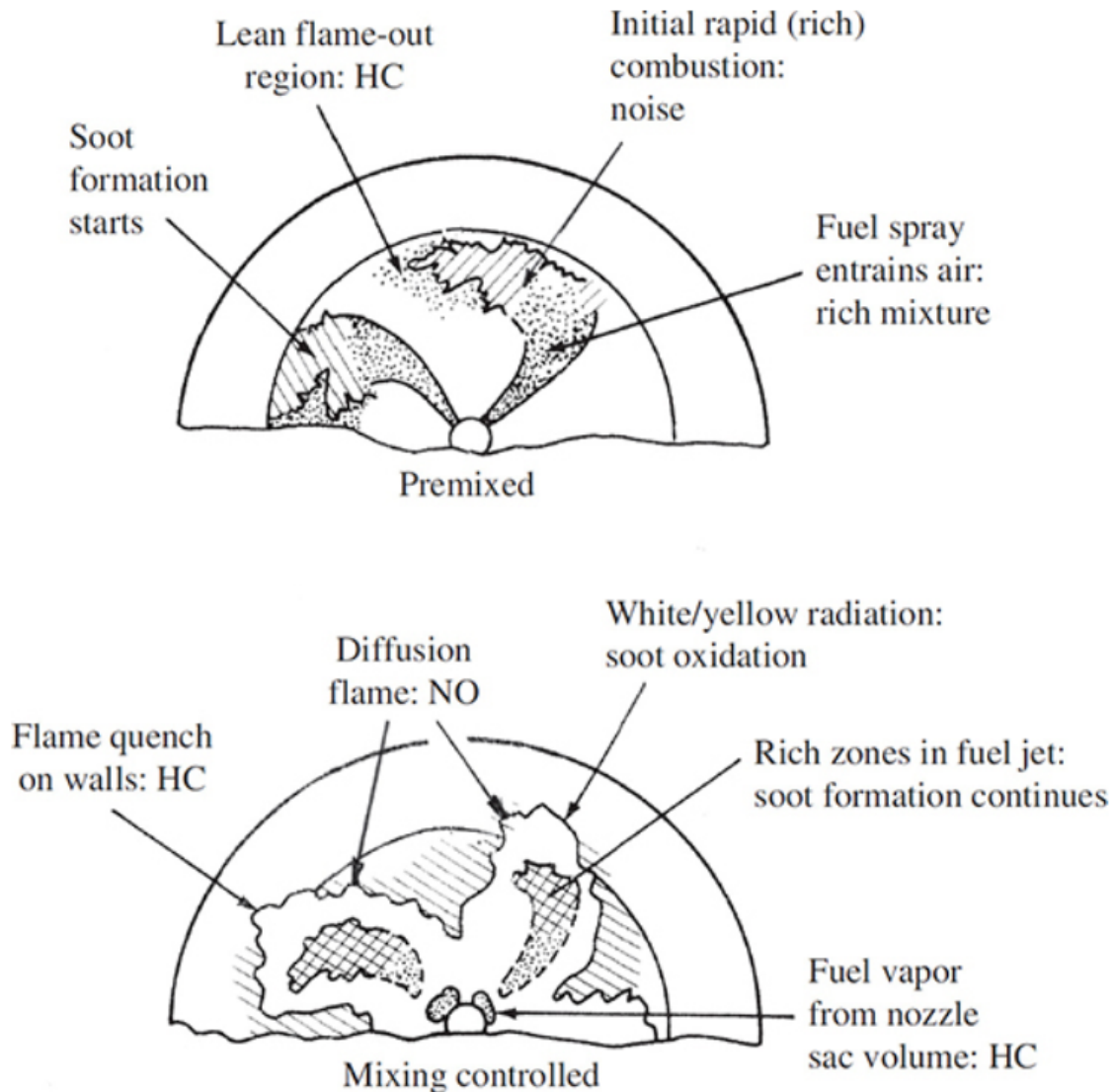


FIGURE 1.2: Pollutant formation during pre-mixed and mixing-controlled phases of diesel combustion.

The chemical reaction represented in Eqn.(1.2) has an extremely high activation energy, thus resulting in a high sensitivity to temperature. Therefore, this mechanism is very important at higher temperature and at air/fuel mixtures that are close to stoichiometric. The contribution to  $NO_x$  emissions is almost insignificant at temperatures below 1700 K, but is strongly accelerated as temperature increases above 2000 K.

NO can then be rapidly converted to  $NO_2$  via reaction represented in Eqn.(1.5).



A work conducted at General Motors in the 1980s suggested that the premixed burning phase of the diesel combustion process occurs under very fuel rich conditions, under which very little  $NO_x$  actually forms due to low oxygen concentrations and low temperatures, and the

diffusion burning region is indeed the primary source of  $NO_x$  [2].

Even though  $NO_x$  formation during premixed combustion is low, the burned  $NO$ , when compressed inside the combustion chamber, reaches the highest temperature of any portion of the cylinder charge and forms localised heat pockets. For this reason, the techniques to control  $NO_x$  focus on this early phase of diesel combustion.

## 1.4 Legislation

The  $NO_x$  emissions from diesel engines cause inflammation to the human respiratory tract and have adverse effects on human health [3]. Additionally,  $NO_x$  forms Nitric acid after reacting with the water vapour present in the atmosphere, which in the form of acid rain causes harm to the ecosystem.

Thus, to reduce the harmful effects of  $NO_x$ , there are limits imposed worldwide on the allowable emissions from vehicles. In the USA, the Federal Test Procedure (*FTP*) heavy-duty transient cycle is currently used for emission testing of heavy-duty on-road engines. The transient test accounts for a variety of heavy-duty trucks and buses in American cities and also traffic on roads and expressways. The transient cycle represented in Fig. 1.3 consists of four phases:

- New York Non-Freeway (*NYNF*) phase, typical of light urban traffic with frequent stops and starts
- Los Angeles Non-Freeway (*LANF*) phase, typical of crowded urban traffic with few stops
- Los Angeles Freeway (*LAFY*) phase, simulating crowded expressway traffic in Los Angeles
- *NYNF* phase (repeated).

The test procedure comprises a cold start after a parking overnight, followed by idling, acceleration and deceleration phases. The most recent legislative requirements set by the environmental protection agency (*EPA*) require ultra-low  $NO_x$  emissions of 0.02 g/(bhp-h) by 2027, which is a 90% reduction from the current level of 0.2 g/(bhp-h).

## 1.5 $NO_x$ control techniques

The HD industry is investing significant resources in researching alternate fuels, aggressive thermal management, enhancing the conversion efficiency of after-treatment systems and electrified powertrains, to comply with the stringent Ultra-Low  $NO_x$  emission requirements. In this section, some of the widely adopted approaches of  $NO_x$  control in diesel engines will be discussed.

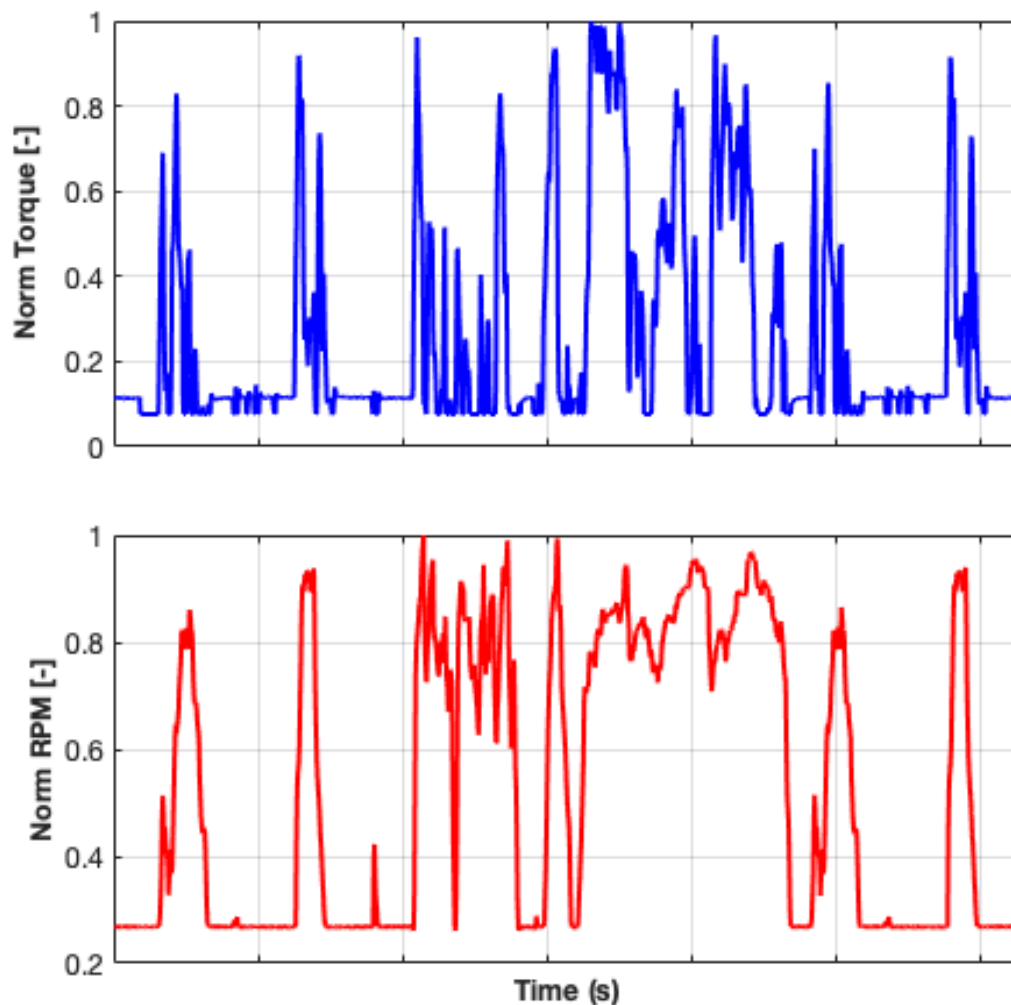


FIGURE 1.3: HD-FTP transient drive cycle

### 1.5.1 In-cylinder NO<sub>x</sub> control techniques

As mentioned in section 1.3, the mixing of air and fuel inside the combustion chamber affects NO<sub>x</sub> formation. Thus, the main engine operating parameters which define the mixture composition and eventually lead to in-cylinder NO<sub>x</sub> control are:

- Air-fuel ratio ( $\lambda$ )
- Turbine boost
- Injection timing
- Exhaust gas recirculation

#### Air Fuel ratio

- NO emissions decrease with increasing  $\lambda$ . The Fig. 1.4 [1] represents NO<sub>x</sub> formation as a function of equivalence ratio  $\frac{1}{\lambda}$ .

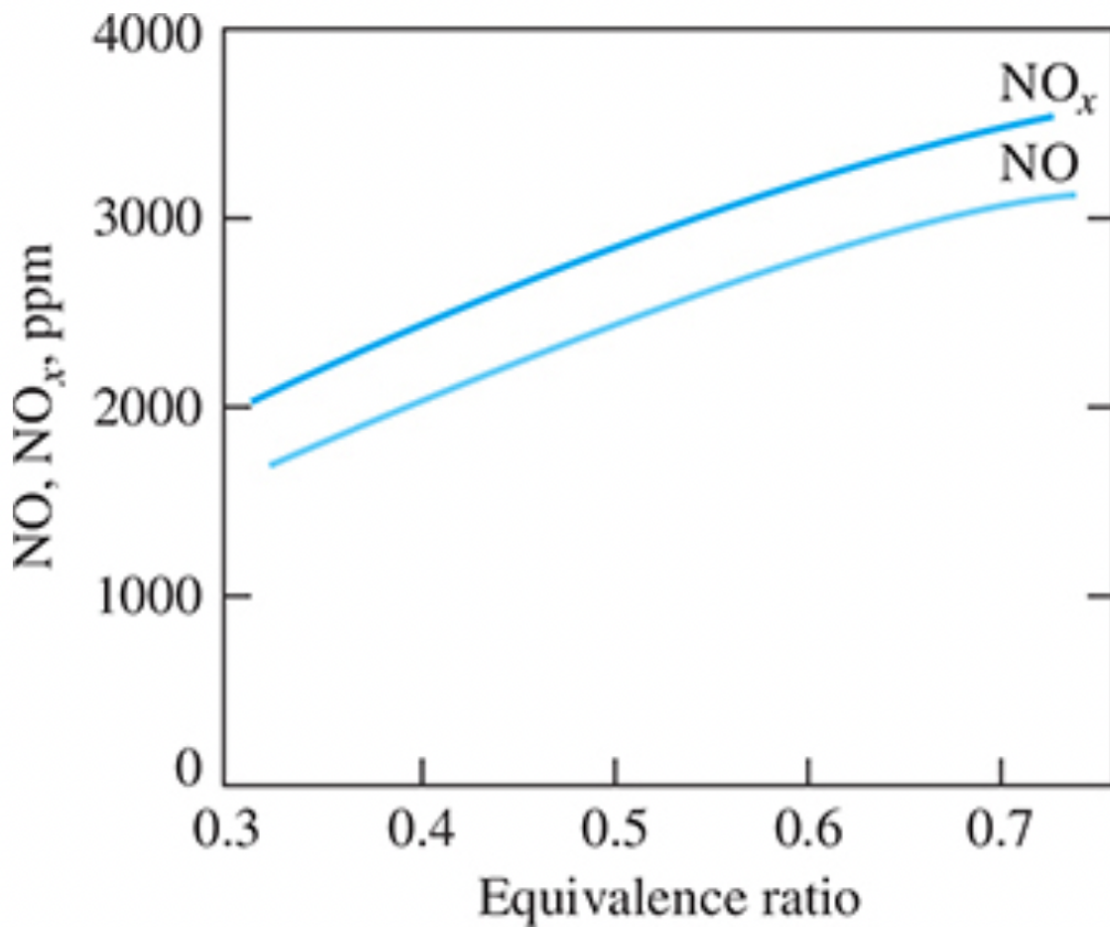


FIGURE 1.4: Effect of equivalence ratio on NO<sub>x</sub> formation.

### Boost

- Introducing compressed air into the intake with the help of a turbocharger unit increases the intake air density. This improves spray development and mixing as the liquid length decreases. Simultaneously, boost also helps accommodate higher EGR rates as the available space within the combustion chamber increases due to higher air density.

### Injection timing

- Injection advance extends the ignition delay, and more fuel can be injected as the temperature is low (during the early compression phase). Thus, there will be a greater premixed portion of the fuel before ignition. On the contrary, if the injection timing is retarded, the ignition delay reduces and lowers the premixed combustion phase, thus resulting in lower *NO* formation.

Though injection timing advance benefits in NO<sub>x</sub> reduction, it negatively affects the fuel economy as depicted in Fig. 1.5 [4].

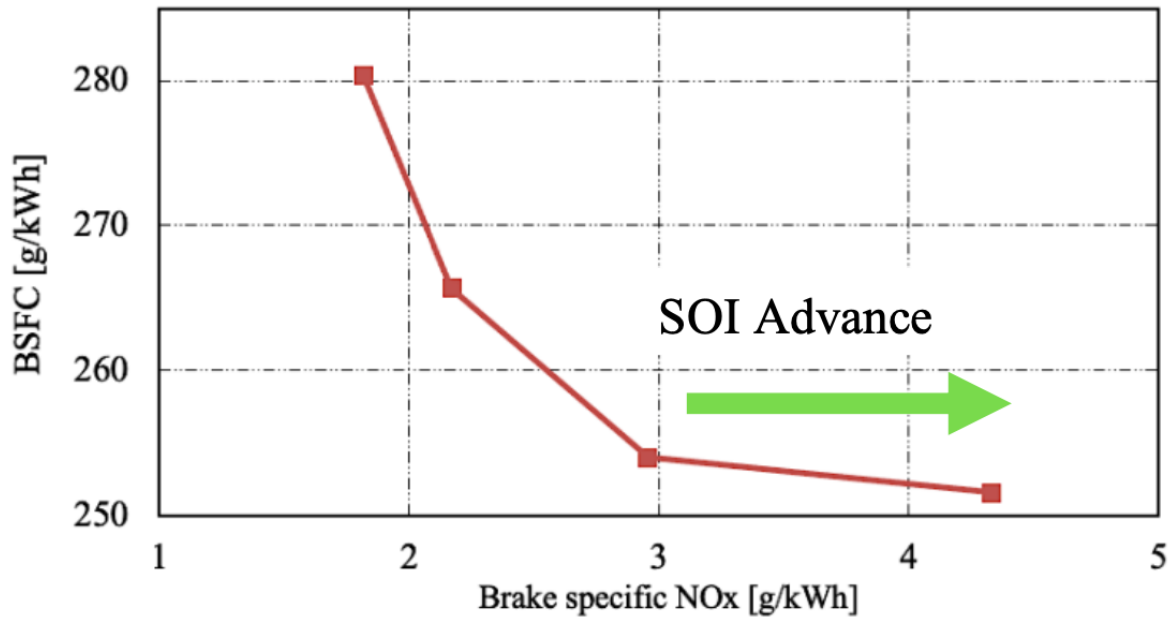


FIGURE 1.5: Effect of injection timing on brake specific NOx emissions and fuel consumption.

### Exhaust gas recirculation

- Inducing exhaust gas back into the intake lowers the amount the fresh air available for combustion. This lowers the in-cylinder temperature and reduces NOx formation. Similar to the case of injection timing, introducing EGR for NOx reduction has a negative impact on soot emissions, as represented in Fig. 1.6 [4].

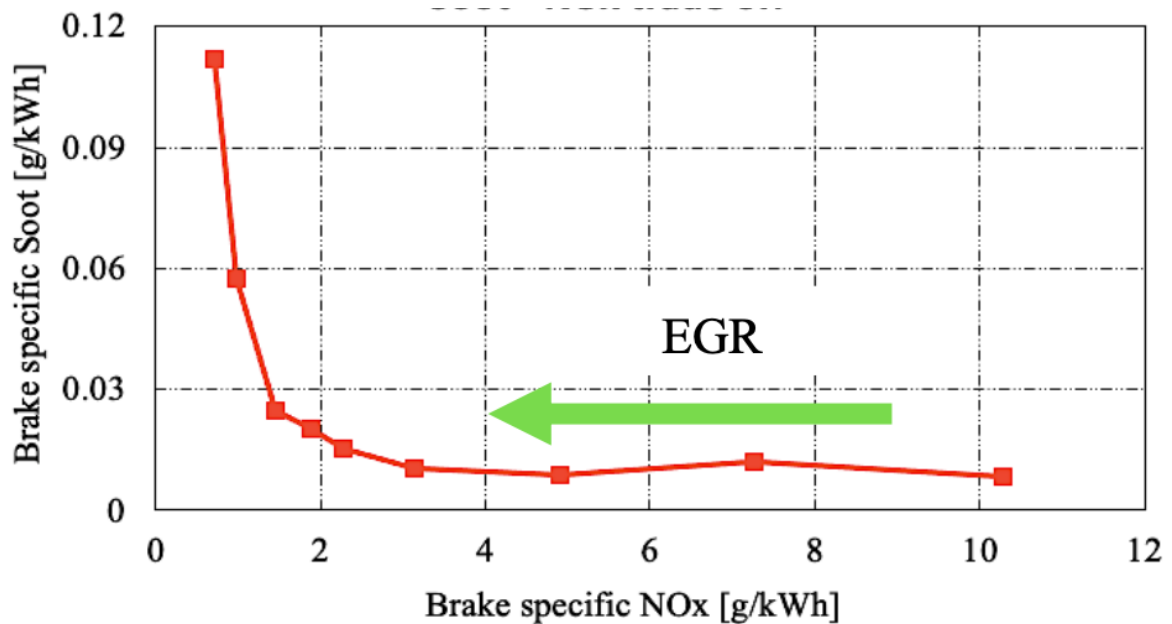


FIGURE 1.6: Effect of EGR on brake specific specific NOx and soot emissions

### 1.5.2 After-treatment systems (NO<sub>x</sub>)

Though, the adoption of in-cylinder NO<sub>x</sub> control techniques are beneficial, they also have negative impacts on the engine performance, in terms of fuel consumption increase, soot formation and inefficient engine operation. Thus, to overcome the limitations of the calibration techniques, external after-treatment devices are used on diesel vehicles. With engine calibration only about 50% reduction in NO<sub>x</sub> emissions can be achieved. However, the usage of after-treatment systems further lowers the NO<sub>x</sub> emissions to about 99%.

In the context of NO<sub>x</sub> emission control, the following systems are found in diesel engines:

- Selection catalytic reduction (SCR) with Ammonia
- SCR with hydrocarbons (DeNO<sub>x</sub> catalysts)
- Lean NO<sub>x</sub> trap

#### Ammonia SCR catalysts

- The SCR is used as an after treatment system to reduce NO<sub>x</sub> emissions by injecting a Diesel Exhaust Fluid (DEF) into a catalyst, in the exhaust line. The injected DEF generates Ammonia (NH<sub>3</sub>) through thermolysis and hydrolysis, which gets deposited on the substrate of the catalyst, where the NO<sub>x</sub> flow and the NO<sub>x</sub> reduction reactions (together with other undesired reactions) take place, depending on the SCR substrate temperature. Fig. 1.7 [1] represents a schematic of the Ammonia SCR system.

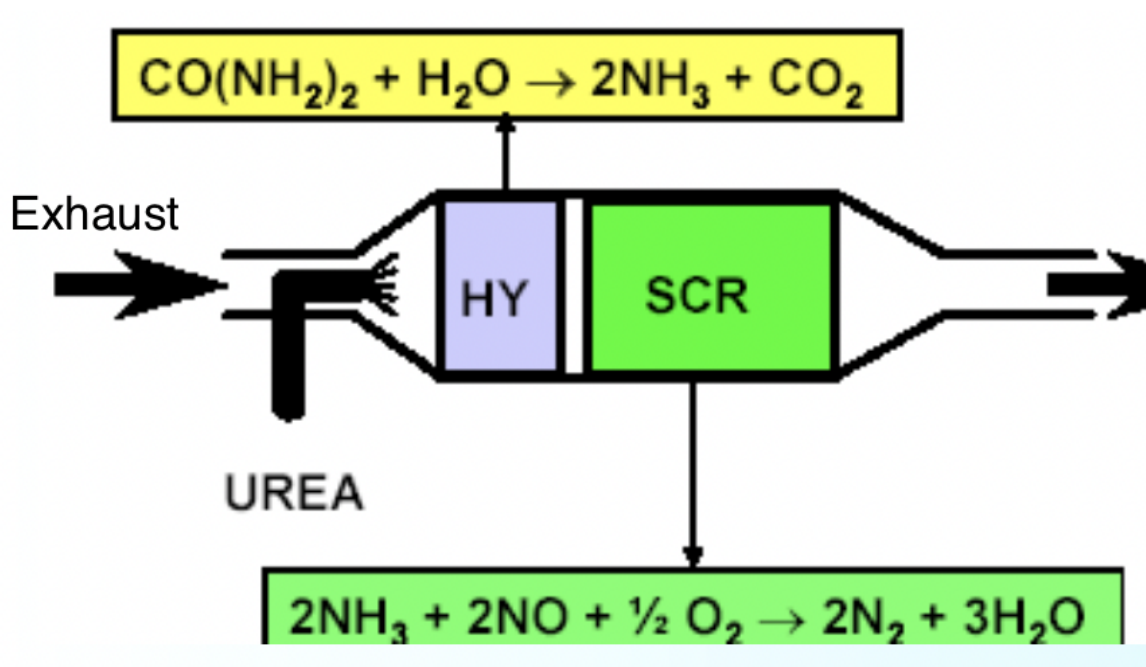
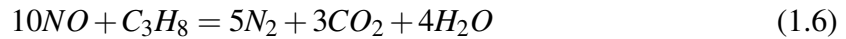


FIGURE 1.7: Working principle schematic of an SCR system.

### DeNOx catalysts

- This technology relies on either using *HCs* and *CO* available in the exhaust (passive DeNOx) or on injecting additional fuel (active DeNOx) for reducing NOx emissions, instead of *NH<sub>3</sub>*, as represented in Eqn.(1.6). NO reduction can be carried out under rich conditions where there is an excess of reducing species. However, the rich operation necessary for NO reduction results in a fuel consumption penalty.



### Lean NOx trap

- This catalyst system absorbs and stores NOx when an oxidizing exhaust gas flows through it. Under lean operating conditions, the platinum catalyst oxidizes the NO in the exhaust gases to *NO<sub>2</sub>*. This is then absorbed and stored as an alkaline-earth nitrate on the catalyst surface [1].

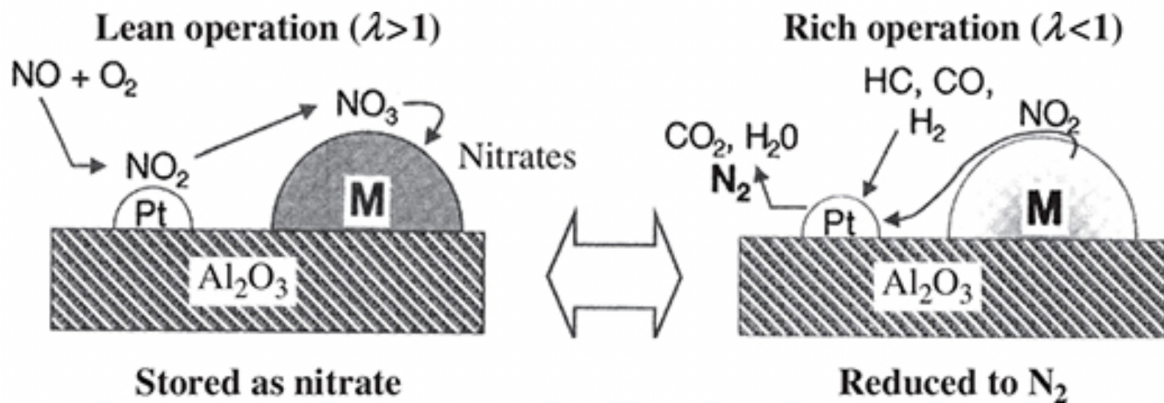


FIGURE 1.8: Operating mechanism of a Lean NOx trap system.

This system has limited storage capacity and thus requires periodic regeneration, usually by introducing purge. During purge, the engine is operated in a fuel-rich condition, so that the exhaust gas constituents can reduce the stored NOx to  $N_2$ .

### 1.5.3 Engine thermal management

Another research area to comply with Ultra-Low NO<sub>x</sub> emission requirements is engine thermal management. Thermal management methods focus on adapting the auxiliary device performance according to engine operation. Fig. 1.9 shows the different thermal management strategies for achieving Ultra-Low NO<sub>x</sub> emissions.

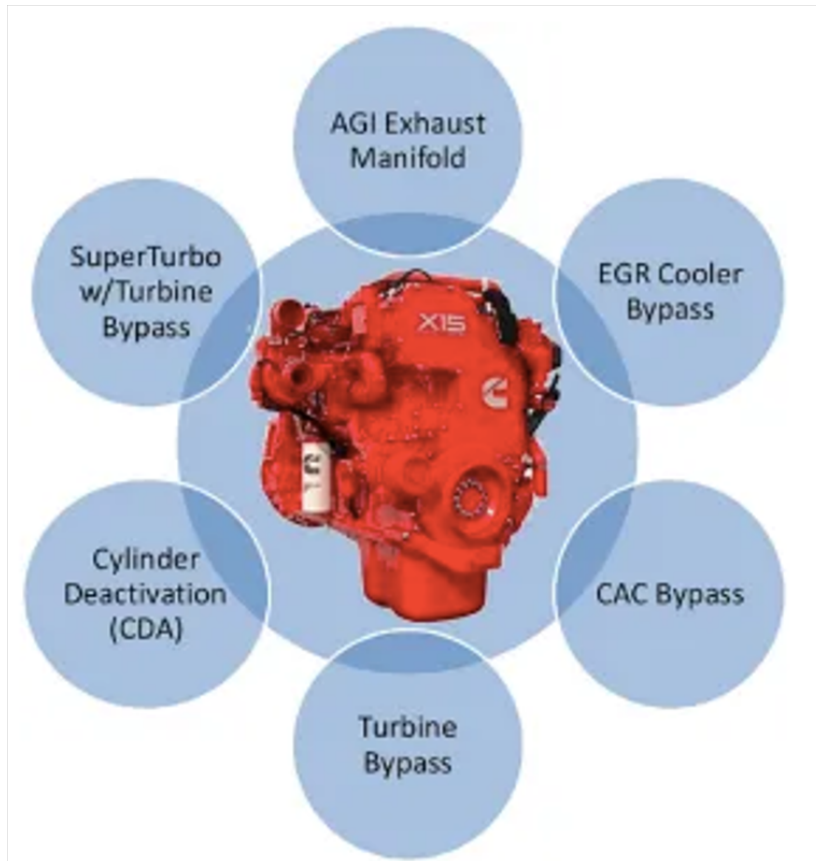


FIGURE 1.9: Various technologies for achieving Ultra-Low NO<sub>x</sub> emissions [5].

#### Cylinder deactivation

- Cylinder deactivation (CDA) technology combines hardware and software computing power to cut off some engine cylinders from an operation based on the power demand, as represented in Fig.1.10. CDA keeps the effective cylinder load in an efficient portion of the engine map. Instead of pumping cold intake air into the exhaust system during coasting or idling, CDA allows the deactivated cylinders to act as springs as the piston moves up and down the bore. CDA causes the active pistons to work harder within a more efficient operating regime, thus increasing fuel economy and generating more heat for faster catalyst warmup.

#### Air cooler and turbine bypass

- Diesel engines incorporate turbochargers for improved performance and EGR to reduce NO<sub>x</sub> emissions, as mentioned in Section 1.5. As the compressed air from the VGT unit

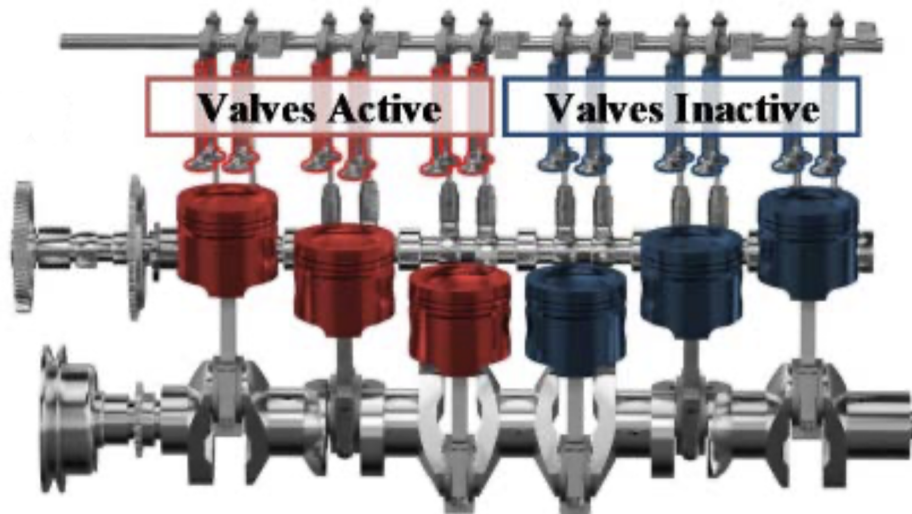


FIGURE 1.10: Cylinder deactivation technology.

and the recirculated exhaust gas are at higher temperatures, they are often cooled before inducting into the intake for performance improvements. For fast catalyst warmup, the EGR gas and compressed air cooling bypass are often adopted, resulting in a hot charge inside the combustion chamber, thus enabling more energy in the exhaust.

## 1.6 Challenges in NO<sub>x</sub> control

Though using exhaust after-treatment systems are widely adopted in diesel engines, these devices can effectively reduce NO<sub>x</sub> only when the catalyst temperature reaches its light-off temperature, typically around 300 deg C [6]. There are two cases when the SCR temperature is low and thus pose a challenge in NO<sub>x</sub> control:

- warm-up period after cold start
- low load operation

During warm-up period after cold start, the SCR temperature is low because of significant heat loss to the ambient. In low load conditions, due to inherently low exhaust gas temperature downstream a turbo (refer Fig. 1.11), SCR can be cooled down below the catalyst light-off temperature. Supplying thermal energy to SCR sufficiently and quickly is a key for fast catalyst light-off. Similarly, the in-cylinder NO<sub>x</sub> control techniques have their short comings in terms of fuel consumption and soot emission, as discussed in section 1.5.1.

Thus, an optimal NO<sub>x</sub> control strategy is needed to provide sufficient thermal energy to SCR while minimizing engine-out NO<sub>x</sub> emissions and fuel consumption, and hence the control problem is multi-objective in nature.

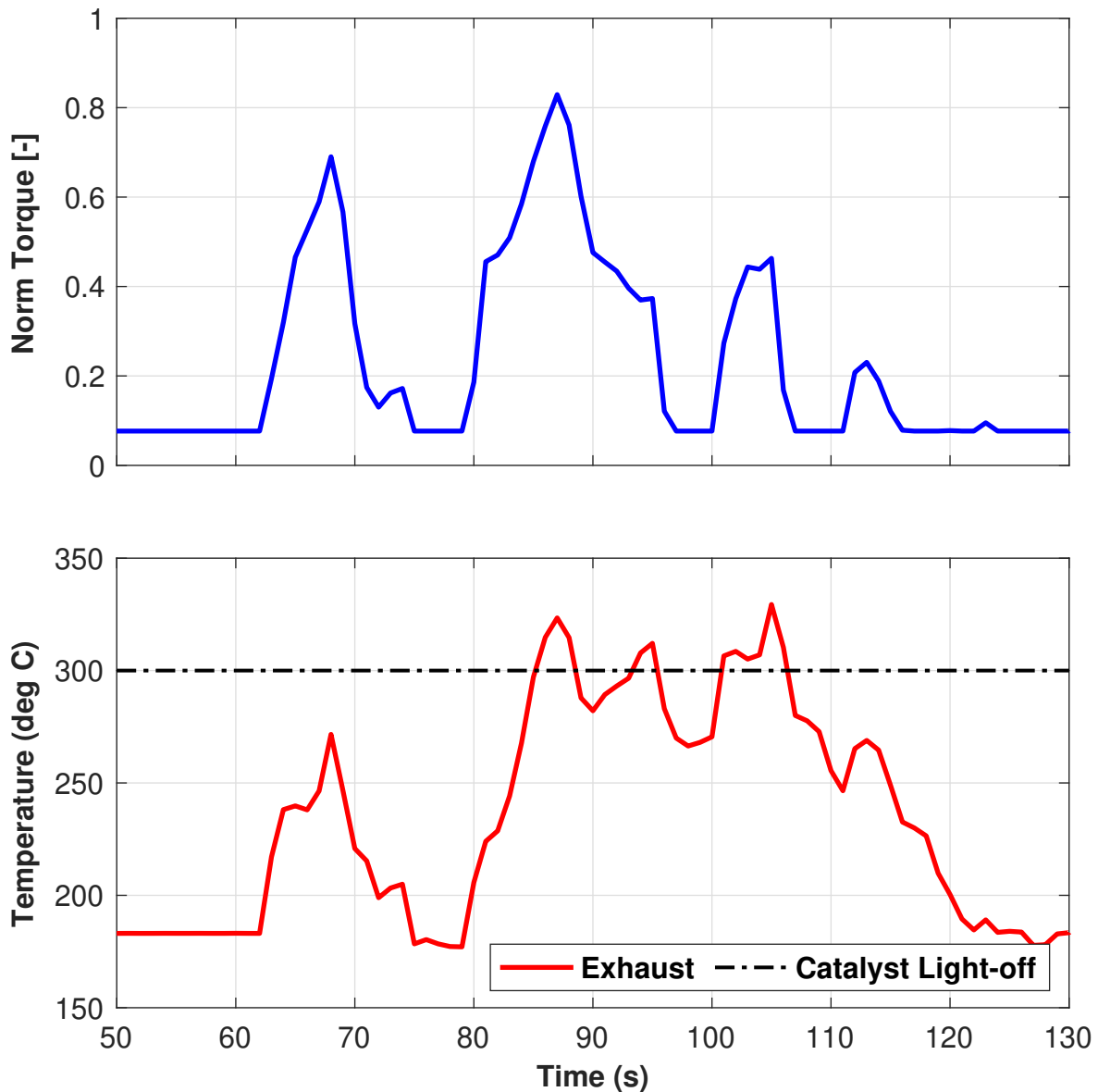


FIGURE 1.11: Map-based HD diesel engine simulation: exhaust gas temperature during low and medium load operation.

## 1.7 Scope of this work

In this work, an optimal control strategy for ultra-low NO<sub>x</sub> compliance of HD diesel engines is addressed. To be specific, the control objective is to reduce engine-out NO<sub>x</sub> emissions and maximize the exhaust thermal energy for fast catalyst light-off during warm-up period and/or low load operating conditions, while ensuring a low fuel consumption and good torque tracking performance. A turbocharged HD diesel engine is considered in control design without any additional hardware. It is equipped with a variable geometry turbo charger (VGT), high-pressure EGR and after-treatment system to improve performance and NO<sub>x</sub> emissions.

Fig. 1.12 depicts the configuration of an in-line HD diesel engine considered in this work.

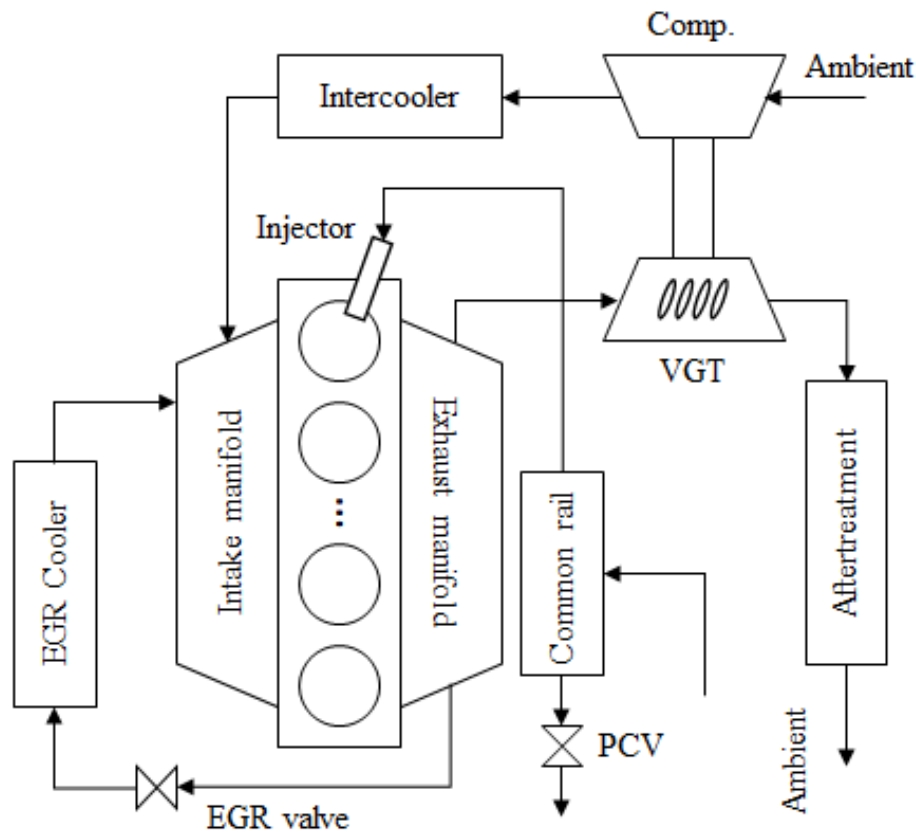


FIGURE 1.12: HD diesel engine configuration: high-pressure EGR, variable geometry turbocharger, after-treatment system (SCR).

Fig. 1.13 shows a hierarchical combustion controller of diesel engines. Given sensor measurements (i.e. engine speed, coolant temperature), a high-level combustion controller finds the desired control commands in physical domain such as fuel flow, fuel pressure and start-of-injection for a fuel system, and charge flow and intake oxygen concentration for an air system. And, low-level controllers in the air and fuel systems control actuators such as injector, common rail, EGR valve and VGT rack position to achieve those desired high-level control commands. The scope of this research is to design an optimal high-level combustion controller to address three conflicting requirements: engine-out NO<sub>x</sub> reduction, fast catalyst light-off and fuel consumption minimization which means an integrated control of a diesel engine and after treatment system implicitly.

This work establishes a method to obtain a globally optimal control sequence of high-level control commands: fuel flow, charge flow, intake oxygen percentage and start of injection (SOI), using dynamic programming (DP) [7], [8] to be achieved by low-level controllers. This work also demonstrates the calibration capability of the optimal controller by simply tuning the weights associated with the parameters in the cost function.

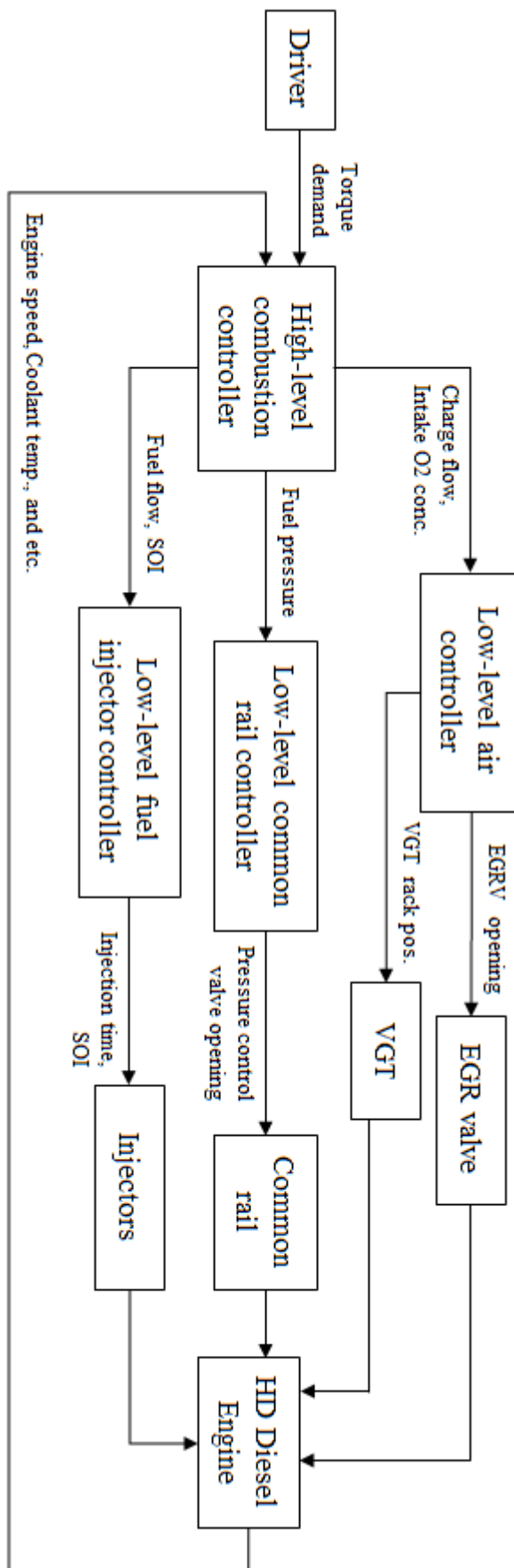


FIGURE 1.13: Controller hierarchy representation of a diesel engine.

## Chapter 2

# Diesel engine simulation model

For the development of this thesis, a Cummins 6.7-Litre six-cylinder engine was referred for sizing, as represented in Table.2.1. The engine models and performance analyses were carried out in MATLAB Simulink, using the powertrain block set to model the engine and the auxiliary components.

TABLE 2.1: Reference engine details

Manufacturer	Cummins
Displacement	6.7 (litre)
Configuration	Inline 6-cylinder
Rated Torque	800 (Nm)
Speed limit	2800 (rpm)

As the work focuses primarily on developing a high-level controller, 15000 engine performance points at different operating conditions were generated using a Full Factorial approach. The performance data from the DOE will be used for obtaining a control-oriented model of the diesel engine using Neural networks and polynomial functions. The details of control-oriented models and the methodology are explained in Chapter.3 of this report.

### 2.1 Resizing engine and performance maps

As the engine performance data from bench tests were not available, a CI dynamometer reference application [9] was referred for collecting the engine performance maps. This application was developed by Mathworks in collaboration with Gamma technologies, using detailed maps from bench testing of a 1.5 L four-cylinder diesel engine. The application can rescale the engine performance data for any diesel engine by simply taking user inputs for desired displacement and number of cylinders (6.7 litre 6-cylinder engine for this work). The application interface of the rescaled engine application is depicted in Fig.2.1.

The rescaled engine Power for a 6.7 L 6-cylinder engine is represented in Fig.2.2. The rescaled performance maps from the dynamometer application are used within the core CI engine block and fluid flow blocks for exhaust and intake manifolds, available in the powertrain blockset.

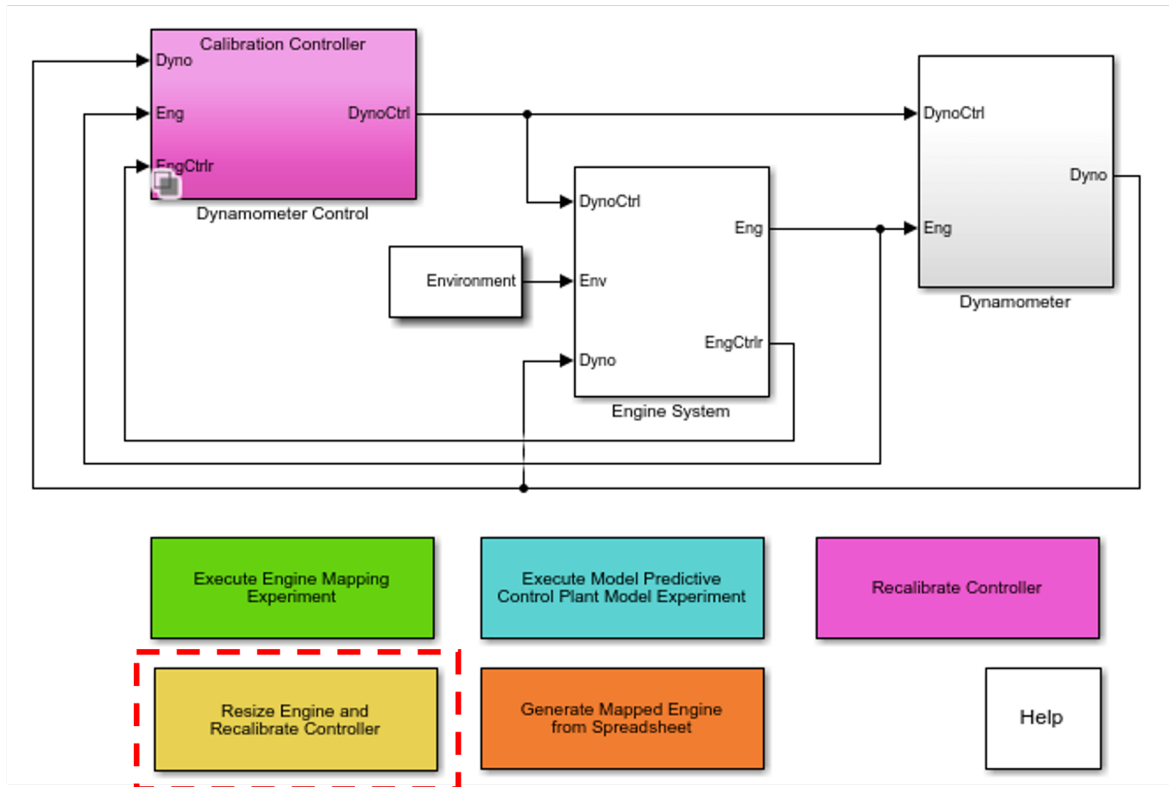


FIGURE 2.1: Mathworks CI engine dynamometer reference application.

Default engine	Rescaled engine
Power or displacement: Displacement	Power or displacement: Displacement
Desired displacement [L]: 1.5	Desired displacement [L]: 6.7
Desired number of cylinders: 4	Desired number of cylinders: 6
Resize Engine	Resize Engine
Current Engine Design	Current Engine Design
Maximum power [kW]: 103.7766	Maximum power [kW]: 322.1951
Number of cylinders: 4	Number of cylinders: 6
Engine displacement [L]: 1.5	Engine displacement [L]: 6.7

FIGURE 2.2: Rescaled engine specification for a 6.7 litre diesel engine.

The engine block evaluates engine torque ( $T_e$ ) using the torque structure model based on fuel mass ( $F_i$ ), SOI, engine speed ( $N_e$ ), coolant temperature ( $T_c$ ), fuel pressure ( $P_f$ ), intake air flow rate ( $m_a$ ) and burned gas ( $m_b$ ) inside the combustion chamber.

$$T_e = f(N_e, F_i, SOI, P_f, m_a, m_b, T_c) \quad (2.1)$$

The engine-out emissions are estimated from the exhaust flow rate ( $m_{exh}$ ), evaluated as the sum of intake air flow rate ( $m_a$ ) and fuel mass flow rates ( $m_f$ ). The pollutant mass fractions ( $Y_i$ ) in the exhaust are evaluated as functions of  $N_e$  and  $T_e$ .

$$m_{exh} = m_a + m_f \quad (2.2)$$

$$Y_i = f(N_e, T_e) \quad (2.3)$$

## 2.2 Design of experiments

To obtain the steady-state performance points of the diesel engine, 15000 data points were simulated over the complete engine operational range using a Latin hypercube sampling technique.

### 2.2.1 Latin Hypercube sampling

Latin hypercube sampling (*LHS*) is a statistical method for generating a near-random sample of parameter values from a multidimensional distribution [10]. A Latin hypercube is the generalisation of the concept of Latin square to an arbitrary number of dimensions, whereby each sample is the only one in each axis-aligned hyperplane containing it.

In LHS, while sampling a function of  $N$  variables, the range of each variable is divided into  $M$  equally probable intervals, which are then placed such that each sample point is unique, thus forcing the number of divisions,  $M$ , to be equal for each variable.

This scheme does not require more samples for an increase in dimensions (variables), and this is one of the main advantages of adopting LHS technique. In LHS, another advantage is that random samples can be taken one at a time, remembering which samples were taken so far, thus resulting in unique samples over the entire range for each variable.

### 2.2.2 Sampling Engine Operational Points

The sampling was performed using the LHS DoE generator Matlab application [11] for different combinations of  $N_e$ ,  $F_i$ ,  $SOI$ ,  $VGT$  rack position and  $EGR$  valve opening percentage, over their operating ranges represented in Table.2.2.

TABLE 2.2: DoE variable operating ranges

Variable	Minimum	Maximum
$F_i(\text{mg})$	10	130
$N_e(\text{RPM})$	800	2800
VGT rack	0	1
EGRvalve(%)	0	20
SOI( $^{\circ}\text{CA}$ )	-10.5	1.5

Though the fuel injection pressure is crucial for emission formation and combustion, it was considered constant in developing this work, due to limited modelling capabilities. The samples (2000 for illustration) of  $N_e$  and  $F_i$  obtained using the Matlab application are represented in Fig.2.3. The engine simulation model and layout for this study are represented

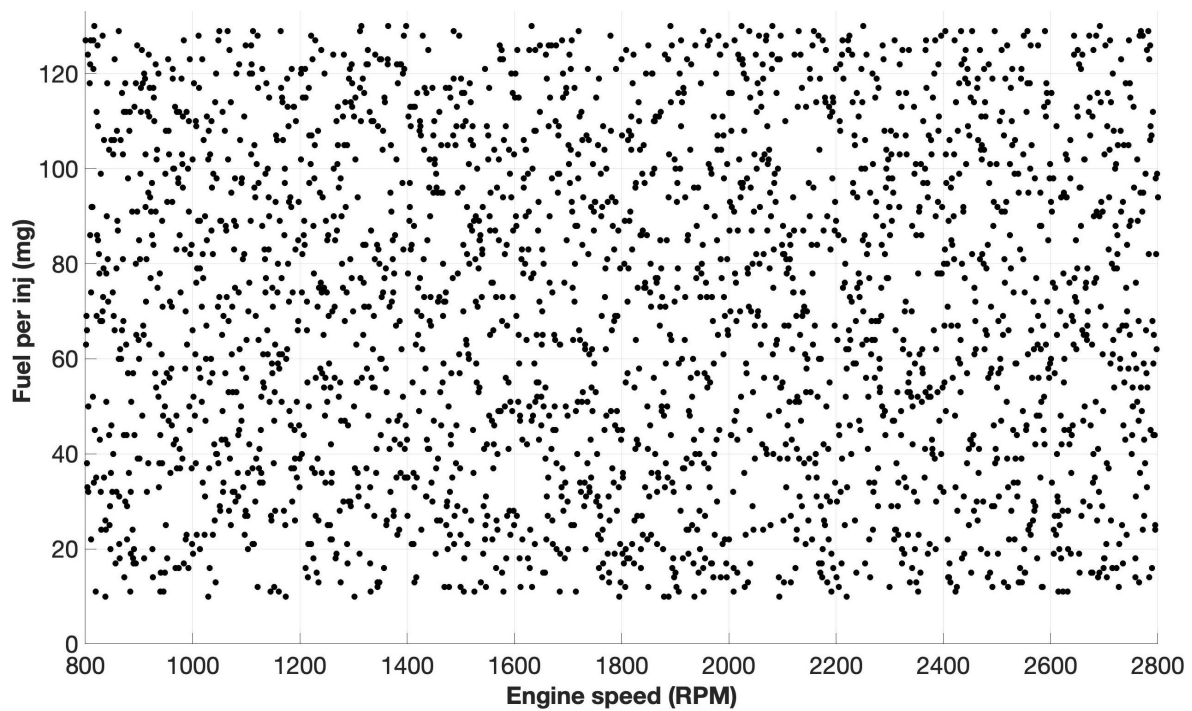


FIGURE 2.3: Unique samples of Fuel mass & RPM obtained using LHS DoE generator.

in Fig.2.4.

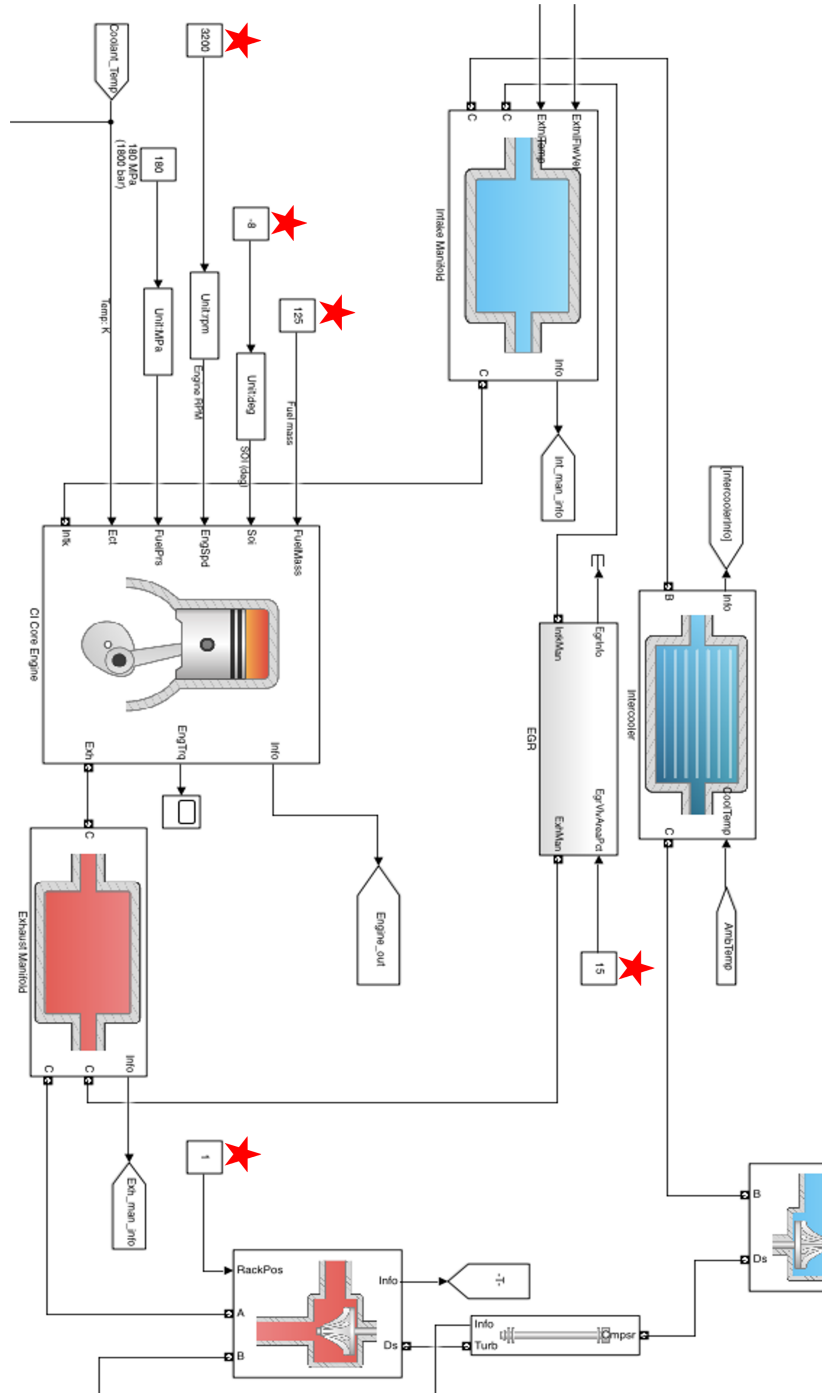


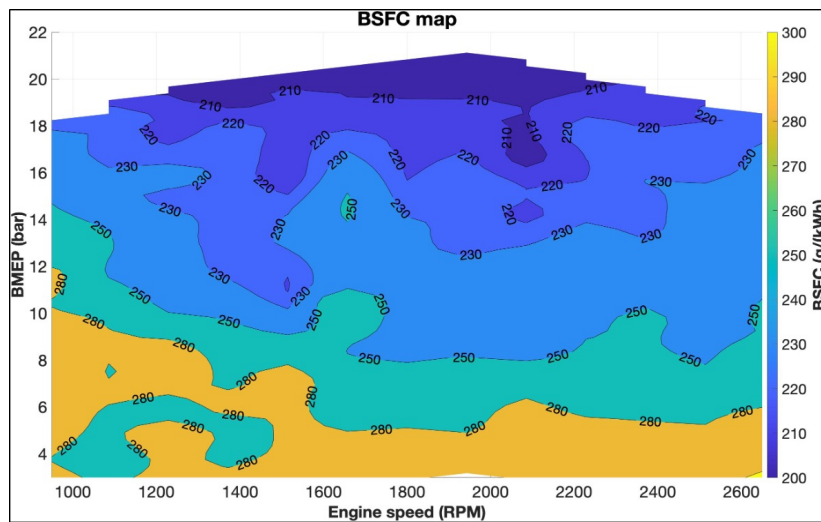
FIGURE 2.4: Engine simulation model and layout.

## 2.3 Engine performance plots

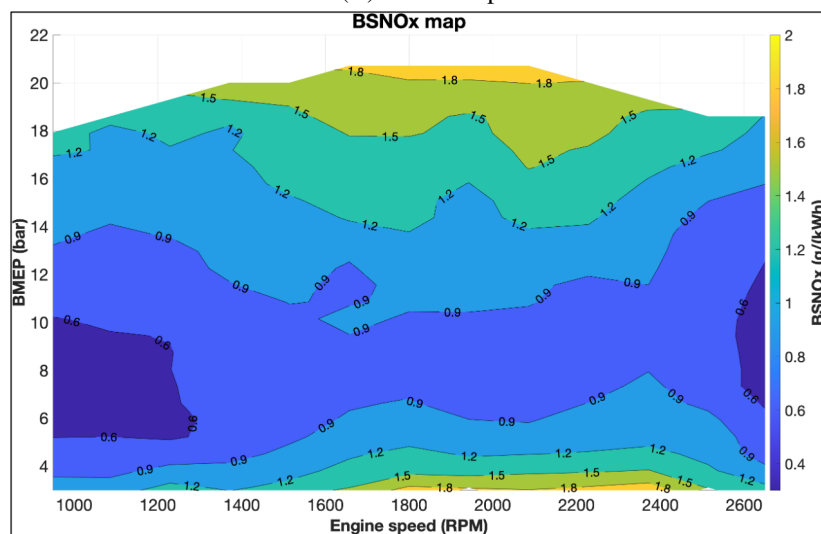
In this work, each of the 15000 experiments was run for 10 seconds to obtain steady-state engine response, exemplifying engine testing on a test bench. For each experiment, the following performance parameters were logged, which will later be used for obtaining the control-oriented model:

- $T_e$
- $N_e$
- $m_f$
- Charge flow rate ( $m_c$ )
- $O_2\%$
- SOI
- NOx emissions
- Exhaust enthalpy

The fuel consumption and NOx emission maps as a function of engine load, characterized by brake mean effective pressure ( $BMEP$ ) and engine speed are represented in Fig.2.5.



(A) BSFC map



(B) BSNOx map

FIGURE 2.5: Steady state DoE performance plots

## Chapter 3

# Control oriented model

### 3.1 Background

In control studies, tuning the control gains and weights is an iterative process. However, running numerous tests on the engine test bed is infeasible due to the high development time, and the cost of development increases substantially with the increase in the number of calibration iterations. With today's need to significantly reduce NOx emissions, the control studies are performed on virtual engine models instead of physical tests. The classification of engine modelling approaches falls broadly into three main categories [12]:

- Phenomenological models
- Empirical models
- Semi-empirical models

#### 3.1.1 Phenomenological Models

The Phenomenological models calculate the in-cylinder NOx levels based on the detailed numerical models that describe the evolution of thermodynamics and chemical species formation during combustion. These models adopt quasi-dimensional or zero-dimensional thermodynamic modelling methods for diesel flame development and detailed 3D computational flow models for charge motion.

#### 3.1.2 Empirical Models

Empirical models rely on the measured data to identify relevant correlations for predicting NOx emissions. They have the advantage of requiring a low computational effort without detailed knowledge of the physical or chemical processes in the combustion chamber. However, these empirical models usually show a good predictive performance in the calibration range used for training. Thus, their application is limited as they are not physically consistent for engine operation outside the training region.

#### 3.1.3 Semi-Empirical Models

Semi-empirical models usually combine the physical and chemical parameters related to the NOx formation process with the relevant engine operating parameters that can be directly measured or evaluated, as in the case of empirical models. Semi-empirical models have the

advantage of a lower computational load than phenomenological models and are more physically consistent and accurate than empirical models. Moreover, semi-empirical models are reliable over a wide range of engine operation conditions [13], [14], [15], [16].

Over the years, Artificial Neural Networks (*ANN*) have become a new domain of interest for engineers in the automotive sector. The new-found interest is because of their ability to model complex non linearities between multiple inputs and multiple output (*MIMO*) systems, even with less test data availability [17].

Hence, feed-forward type Artificial Neural networks (*ANN*) were adopted to obtain the control-oriented diesel combustion model for developing this research work. However, due to some incompatibility (specific to this work) of *ANN* with Dynamic Programming (*DP*) for a global-optimal solution (chapter 4), a multi-variable polynomial regression model was later adopted for obtaining the engine model.

### 3.2 Multi Layer Perceptron Neural Networks

A multi-layer perceptron (*MLP*) network is a feed-forward type network consisting of an input layer, an output layer, and several hidden layers, each with a certain number of nodes, as depicted in Fig.3.1), each known as a perceptron. In an *MLP* architecture, all nodes of one layer are fully connected with the nodes of the subsequent layer, and the computation takes place from the input layer to the output layer [18].

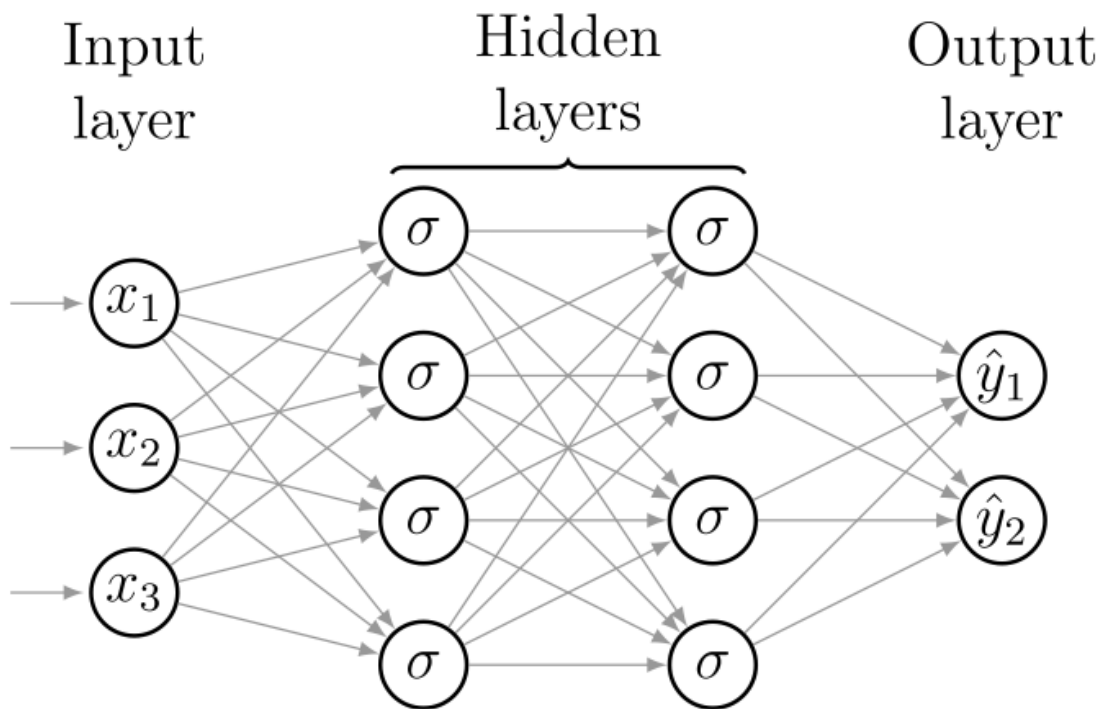


FIGURE 3.1: Feed-forward type neural networks with fully connected nodes [19].

The elements in the input layer are multiplied by a weight matrix, and then a bias vector is added. The outcome then propagates to the hidden layers. The number of hidden layers is crucial for determining the prediction accuracy of the network. However, adding too many layers may result in over-fitting. Non linear activation functions are used in between layers to introduce non-linearities in the network which are essential to represent the non-linear behaviour of the input data. Fig.3.2 represents the nodal calculations that occur at a single perceptron.

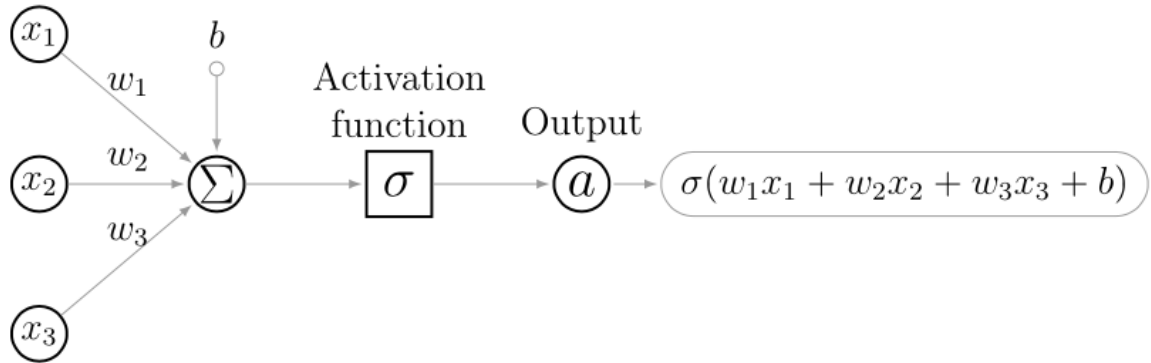


FIGURE 3.2: Representation of network computations in a neural network [19].

The NN model performance is improved based on the mean squared error ( $MSE$ ), and is evaluated using the network prediction  $\hat{y}$  and training input  $y$ , which is back-propagated to update network weights and biases.

$$MSE = \frac{1}{n} \sum_{k=1}^n (\hat{y} - y)^2 \quad (3.1)$$

where  $n$  represents the number of samples.

### 3.3 Multi-Variable Polynomial Regression

In multi-variable polynomial modelling methods, the relationship between independent variables and their responses (dependent variables) is defined using polynomial functions. Polynomial regression models are simple to adopt and require minimal processing. These models can describe complicated relationships in data by increasing the polynomial order. The generic representation of a polynomial function of order  $k$  consisting of multiple independent variables  $x_1, x_2, \dots, x_j$  and an output  $y$  is shown in Eqn.3.2.

$$y = \beta_0 + \beta_1 x_1 + \beta_2 x_1 x_2 + \beta_3 x_1^2 + \dots + \beta_n x_j^k \quad (3.2)$$

where  $n$  represents the number of polynomial terms.

### 3.4 Control-Oriented HD Diesel engine Model

The development of the diesel engine combustion model is carried out using two modelling approaches, as mentioned in the previous section:

- Artificial Neural Networks
- Multi-Variable Polynomial Regression

For each of these approaches, the model input is a vector containing to the model vector containing  $N_e, T_c, m_f, m_c, O_2\%, SOI$ , as explained in section 3.2 on page 22.

#### 3.4.1 Neural Network model

##### Network Architecture

This work focuses on developing a neural network representing the diesel engine, consisting of an input layer, an output and a hidden layer of fully connected nodes. The input layer consists of six high-level engine parameters and generates  $T_e$ , NOx flow rate ( $m_{NOx}$ ) and exhaust specific enthalpy ( $E$ ).

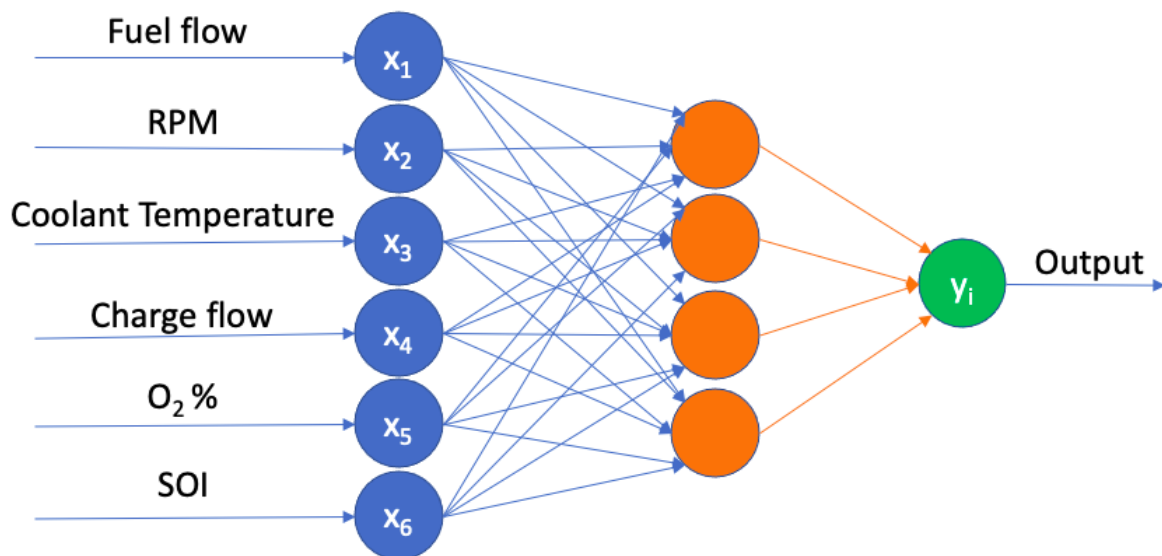


FIGURE 3.3: Neural network model of HD Diesel Engine.

##### Training

The neural network was trained using 15000 steady-state operating points, obtained from the *DoE* activity. The models are developed using the MATLAB deep learning toolbox. The neural network tool randomly selected 80% of the data points for model training and 20% for testing. The decision for the network training algorithm and the number of hidden layer nodes was based on a nodal sensitivity study. Two different algorithms, i.e., Levenberg Marquardt and Bayesian regularisation, were adopted for obtaining the neural networks by

varying the nodes from 5 to 15.

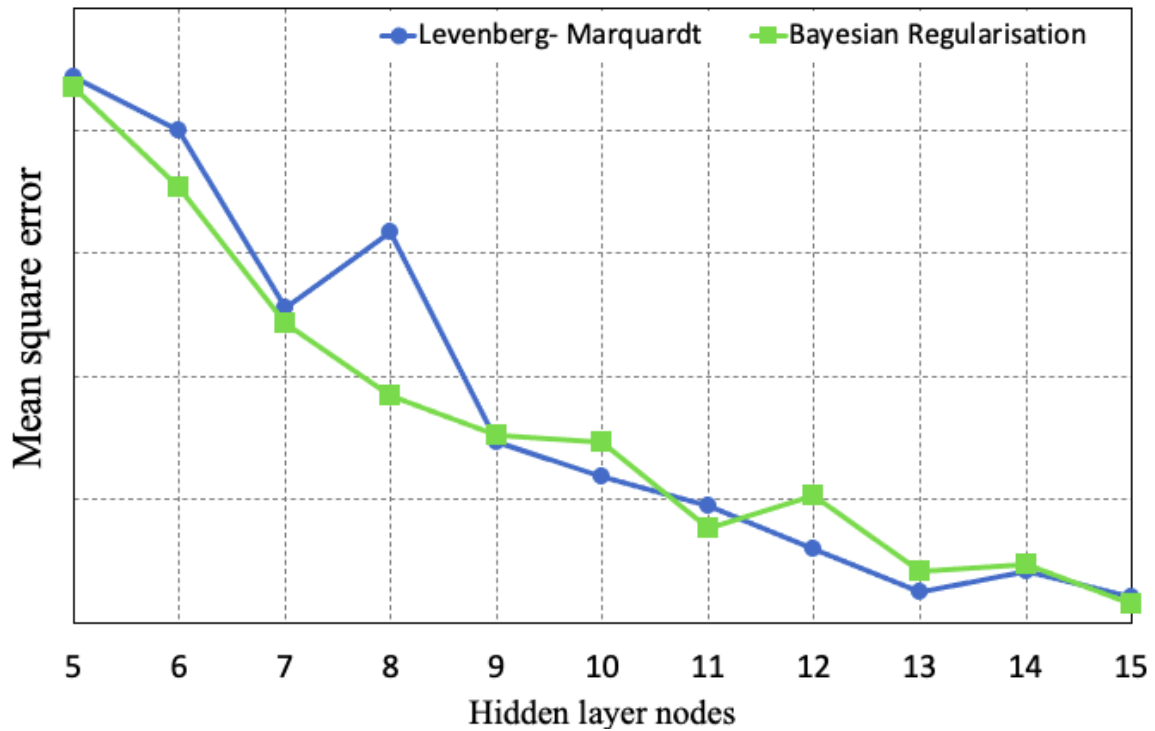


FIGURE 3.4: Sensitivity analysis of NN Model prediction as a function of hidden layer nodes.

Even though the MSE decreases as the number of hidden layer nodes increases, suggesting model performance improvement, the computational time also increases. Thus, the selection of hidden layer nodes is a trade-off between model accuracy and computation. However, the literature suggests that for engine emissions control and performance modelling studies, neural networks of up to 10 hidden layer nodes are sufficient to model the system behaviour [20].

### Model Performance

The NN models from steady-state engine performance data were analysed on the HD-FTP drive cycle for transient performance capabilities, essential for optimal control studies. In this work, the networks trained using the Bayesian regularisation algorithm were more effective in predicting engine responses on the HD-FTP drive cycle than those obtained using the Levenberg-Marquardt algorithm. The performance comparison for different configurations (number of hidden layer nodes) of NN models is shown in Fig.3.5. The model consisting of five hidden layer nodes generated the best transient performance for predicting  $T_e$ , and models with seven hidden layer nodes yielded the best modelling accuracy for  $m_{NO_x}$  and  $E$ .

Parameter	Algorithm	Nodes	R <sup>2</sup> Value			Best fit (Dynamic performance)		
			Training	Testing	Overall			
Torque	Levenberg - Marquardt	5	0.9982	0.9981	0.9981			
		6	0.9981	0.9980	0.9981			
		7	0.9983	0.9984	0.9983			
		8	0.9983	0.9948	0.9983			
		9	0.9992	0.9989	0.9992			
		10	0.9993	0.9994	0.9993			
	Bayesian regularisation	5	0.9982	0.9976	0.9982		Best fit	
		6	0.9990	0.9991	0.9990			
		7	0.9990	0.9989	0.9990			
		8	0.9991	0.9992	0.9991			
		9	0.9995	0.9994	0.9995			
		10	0.9994	0.9995	0.9994			
NOx	Levenberg - Marquardt	5	0.9942	0.9939	0.9941			
		6	0.9946	0.9951	0.9947			
		7	0.9965	0.9968	0.9966			
		8	0.9969	0.9971	0.9970			
		9	0.9970	0.9963	0.9969			
		10	0.9977	0.9974	0.9977			
	Bayesian regularisation	5	0.9961	0.9955	0.9961			
		6	0.9966	0.9952	0.9966			
		7	0.9972	0.9968	0.9972			Best fit
		8	0.9973	0.9978	0.9973			
		9	0.9975	0.9983	0.9976			
		10	0.9985	0.9978	0.9984			
Exhaust enthalpy	Levenberg - Marquardt	5	0.9960	0.9961	0.9960			
		6	0.9960	0.9961	0.9969			
		7	0.9965	0.9967	0.9965			
		8	0.9984	0.9984	0.9984			
		9	0.9979	0.9978	0.9979			
		10	0.9988	0.9988	0.9988			
	Bayesian regularisation	5	0.9963	0.9964	0.9963			
		6	0.9973	0.9970	0.9973			
		7	0.9974	0.9975	0.9974			Best fit
		8	0.9986	0.9985	0.9986			
		9	0.9989	0.9988	0.9989			
		10	0.9988	0.9989	0.9988			

FIGURE 3.5: NN Model dynamic performance matrix.

It is to be noted that even though the models depicting good transient performance have fewer nodes in the hidden layer (of the analysed configurations), i.e., five for  $T_e$  and seven for  $m_{NOx}$  and  $E$  respectively, the models show similar prediction accuracy on steady-state data, as evident from the  $R^2$  value column in Fig.3.5.

The regression plots for static NN models are shown in Fig.3.6 and the dynamic performance over an HD-FTP cycle is shown in Fig.3.7.

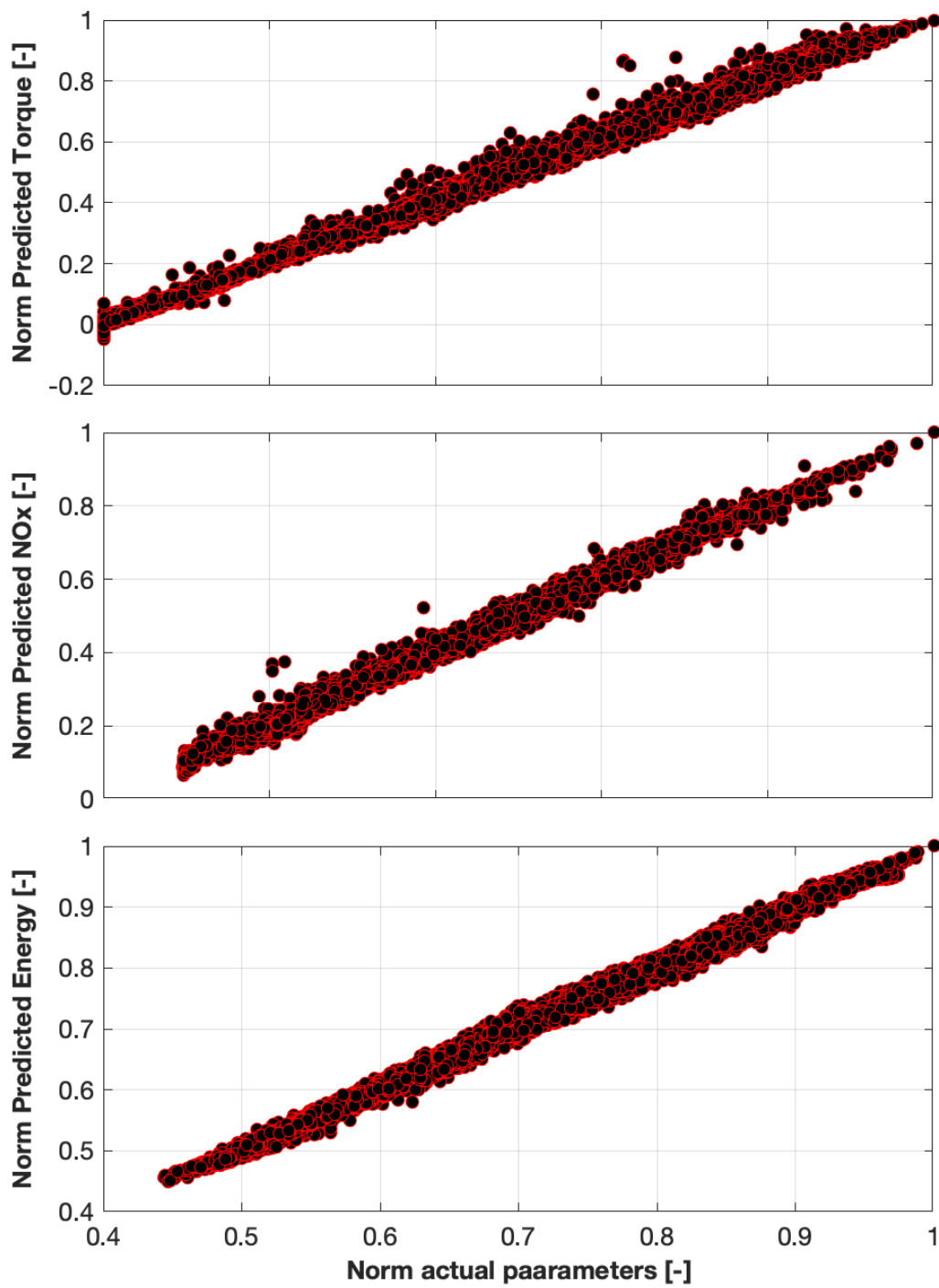


FIGURE 3.6: Neural Network model Regression plots

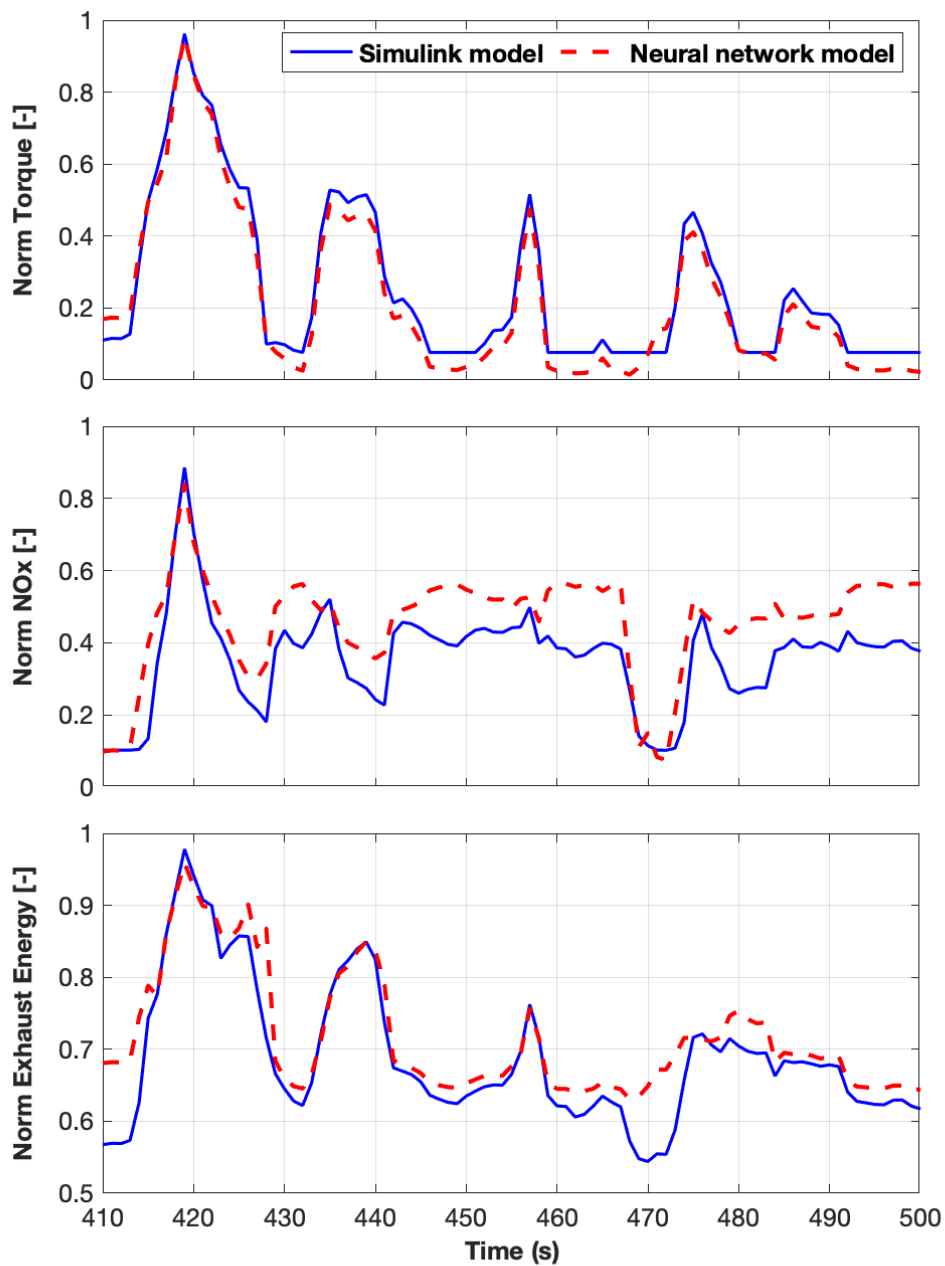


FIGURE 3.7: Neural network model dynamic performance plots

### 3.4.2 Polynomial model

While carrying out the global optimization study using DP (explained in the next chapter), the NN model failed to comply with the dimensional requirements of the DP solver. Hence, a polynomial model for the HD Diesel engine was developed as an alternative to the NN model.

### Model details

For the polynomial model development, the high-level engine performance parameters from the NN model on a transient cycle were considered instead of the steady-state DoE results. The polynomial model for the diesel engine is of second order ( $k = 2$ ) and is mathematically represented as

$$y = \beta_{(i,0)} + \beta_{(i,1)}x_1 + \beta_{(i,2)}x_1x_2 + \beta_{(i,3)}x_1^2 + \dots + \beta_{(i,n)}x_6^k \quad (3.3)$$

where  $x_1, \dots, x_6$  are the control parameters from the input vector  $x$ , and  $y$  is the vector containing engine output parameters, represented as

$$x = \left[ m_f \quad N_e \quad T_c \quad m_c \quad O_2\% \quad \theta_{soi} \right]^T \quad (3.4)$$

$$y = \left[ T_e \quad m_{NOx} \quad E \right]^T \quad (3.5)$$

where  $i$  represents the number of output parameters from the model.

Though the polynomial model was obtained from a pre-trained NN model, it is to be noted that initial model training using the steady-state data was performed but was later terminated to comply with the thesis development timelines. However, the polynomial model training follows a similar approach to the NN model, i.e., the input-output configuration remains the same, and the model performance is improved on the basis of MSE, as shown in Eqn.(3.1).

The model training approach for obtaining a polynomial model is depicted in Fig.3.8.

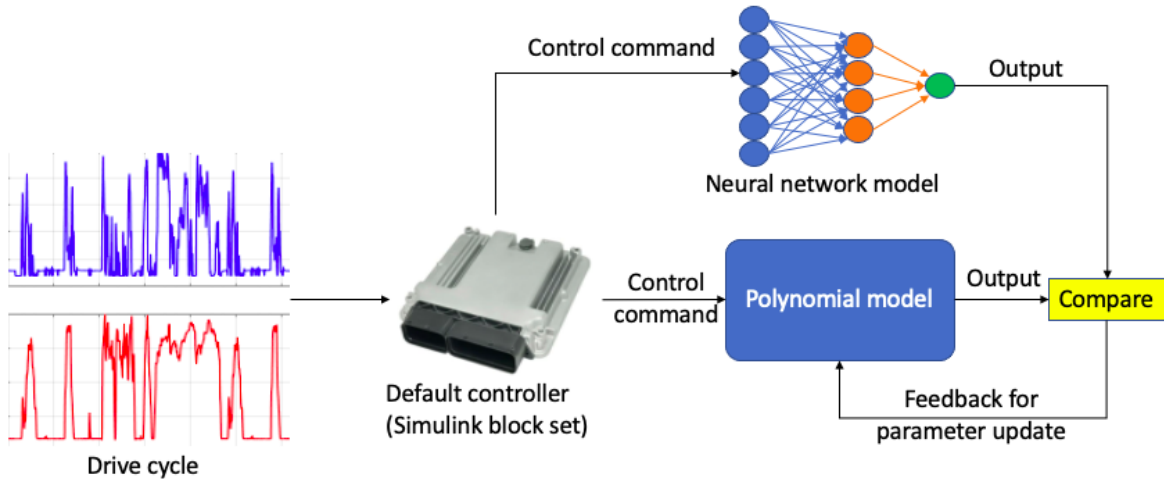


FIGURE 3.8: Polynomial model training flow chart.

For training the model, a default diesel engine controller consisting of rescaled engine maps was used, which takes an external signal for reference Torque and  $N_e$ . The controller then sets input commands for the polynomial model and NN model. Then the outputs are compared to obtain the MSE between predicted (from the Polynomial model) and ground (from the NN model) values. The MSE is then back-propagated for model improvement.

### Model Performance

The polynomial model performance during the transient operation was assessed on an HD-FTP cycle. For comparison, the output of the NN model was used as a benchmark. In this work, it was observed that a polynomial model of  $2^{nd}$  order resulted in a good correlation with the benchmark. The dynamic performance comparison between Polynomial model and the benchmark (NN model) are represented in Fig.3.9. Thus, for the development of a

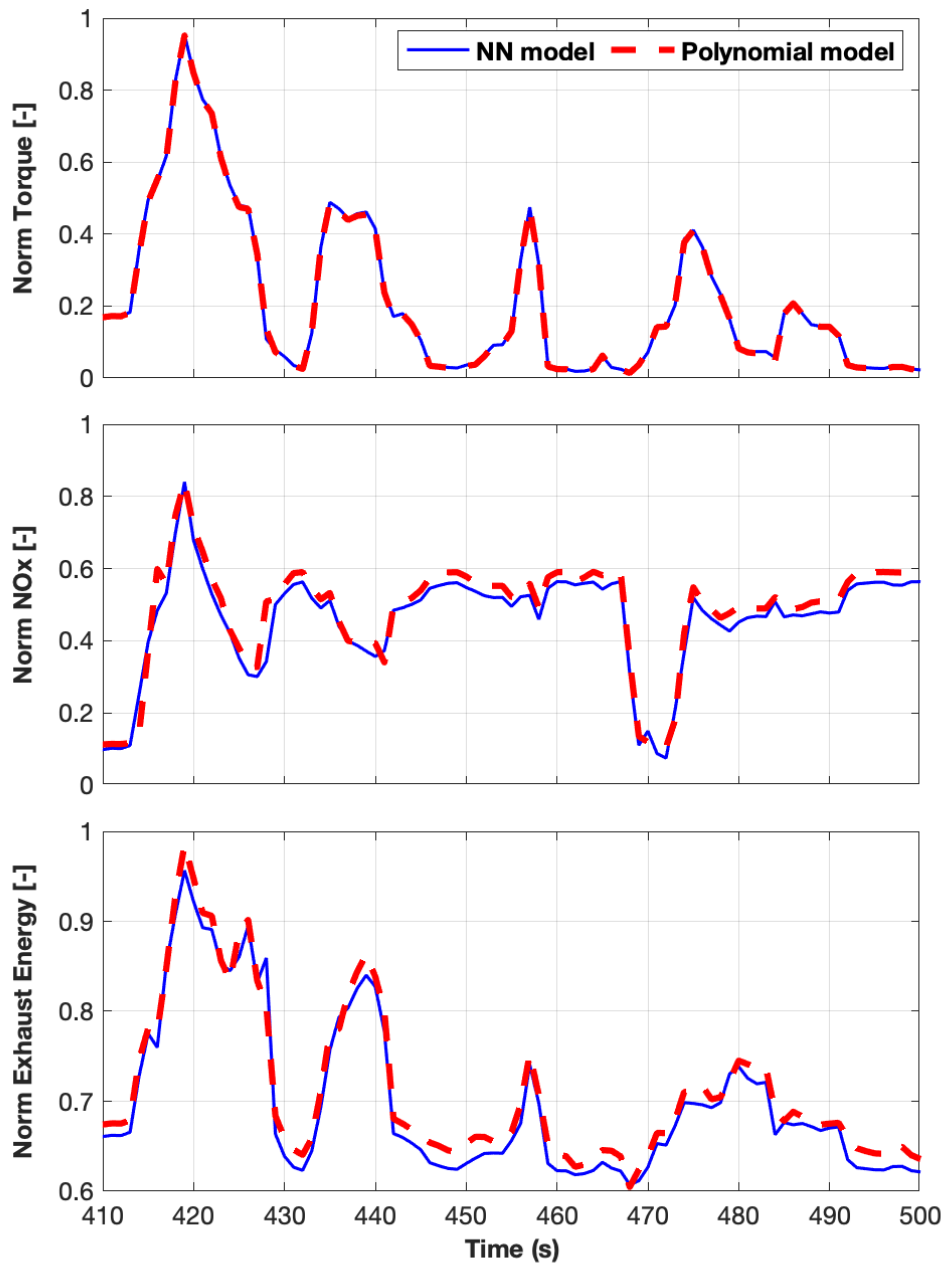


FIGURE 3.9: Polynomial model training flow chart.

global-optimal controller using DP, the diesel engine represented by a  $2^{nd}$  order polynomial functions is used.

## Chapter 4

# Global Optimisation

In this chapter, the methodology for obtaining a global optimal solution for the multi-objective NOx optimization will be discussed. The optimal solution is obtained using Dynamic Programming.

### 4.1 Background

Dynamic programming (*DP*) is a method that, in general, solves optimization problems that involve making a sequence of decisions by determining, for each decision, sub-problems that can be solved. Thus, an optimal solution to the original problem can be found from optimal solutions to sub-problems [21], thus having the ability to generate global-optimal solutions.

DP is widely adopted for optimal control applications with multi-stage decision making [22]. In multi-stage optimisation problems, the objective is often to minimise the cost associated with the problem. The system under study evolves because of its dynamics and external actions, with progressing stages [23]. Thus, for finding optimal solutions to the sub-problems, the optimal control studies that are often of continuous-time type should be discretised for the DP algorithm to evaluate optimal control laws.

Due to its ability to generate global-optimal solutions, DP is being extensively used in the field of energy management in hybrid vehicles [24], diesel emission control [7], and heavy-duty vehicles for fuel consumption optimisation [8]. The application of DP algorithm for optimising fuel consumption is represented in Fig.4.1.

In this work, a Matlab based tool for DP, named Dynaprog [26], is used to obtain the offline controller. The working principle and the limitations associated with the DP optimisation technique, as explained by the developers of Dynaprog are explained in the sections to follow.

#### 4.1.1 Working principle

For achieving a globally optimal control strategy, the DP algorithm estimates the best possible control sequence  $u_k^*$  at each stage  $k$  to minimise the total cost  $J$  incurred over the complete

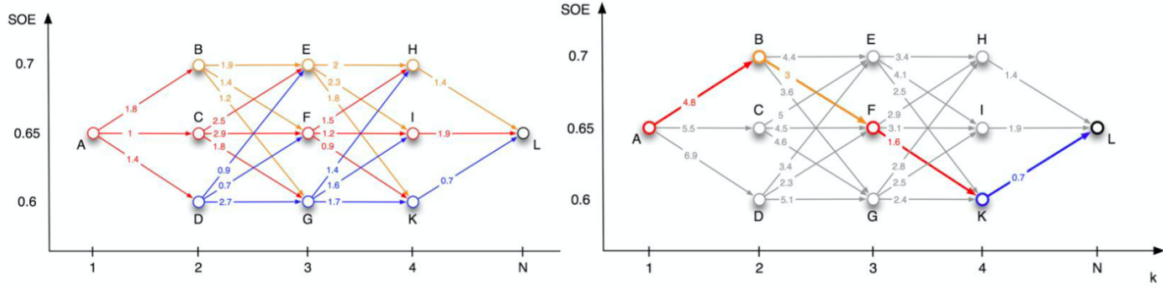


FIGURE 4.1: Dynamic Programming algorithm: study of the possible patterns (left); selection of the pattern related to minimum fuel consumption (right) [25].

process, having  $N$  stages.

$$J(x_0, U_0, \dots, U_{N-1}) = g_N(x_N) + \sum_k^{N-1} g(x_k, U_k) \quad (4.1)$$

where,  $g_N(x_N)$  is the cost associated to the terminal state  $x_N$ . To be more precise, the objective of the DP algorithm is to minimise the stage cost, which is of the form  $g(x_k, U_k)$  and the cost-to-go function  $J_k^*$ , which is the cost associated from stage  $k$  to the final stage, represented as a function of the initial state  $x_k$ .

$$J_k^*(x_k) = \min_{u_k \in U_k(x_k)} (g_k(x_k, u_k) + J_{k+1}^*(f(x_k, u_k))) \quad (4.2)$$

The stage cost and cost-to-go function are evaluated iteratively in the backward simulation. For each stage, the algorithm evaluates the cost-to-go function, based on the initial state and the optimal control sequence for each stage is determined as

$$u_k^*(x_k) = \arg \min_{u_k \in U_k(x_k)} (g_k(x_k, u_k) + J_{k+1}^*(f(x_k, u_k))) \quad (4.3)$$

### 4.1.2 DP Limitations

As mentioned earlier in this chapter, the DP algorithm requires the dynamic system under-study to be discretised to obtain optimal solutions to the sub-problems. Hence, the ability of DP to generate global-optimal solutions to multi-stage control problems is a function of the state and control variable grid resolution. Which is to say, a coarse grid may result in a sub-optimal solution to the control problem, whereas a highly refined grid will result in an exponential rise in computational load [27], making the system unresponsive.

Secondly, the information related to the engine operating cycle should be available a priori. Since the engine operation in the real world is not known beforehand, the application of DP for real-time controller development is not possible. However, DP optimal control solutions are used as benchmarks for control studies performed using other methods.

## 4.2 Problem formulation

In the discussion so far, the working principle of the DP algorithm and a brief background about DP applications were discussed. The key takeaways related to DP are as follows:

- A continuous time should be discretised for optimisation study.
- The main objective of optimisation is to minimise the cost function associated with the control problem.
- The solution optimality depends on the resolution of state and control grids.

Thus, this section focuses on discretising the HD diesel engine model, the state and control input grids and the formulation of the multi-objective cost function for NOx control.

### 4.2.1 Discrete HD Engine model

The combustion model in a discrete state-space form is represented as:

$$x(k+1) = Ax(k) + Bu(k) \quad (4.4)$$

$$y(k) = h(x(k), d(k)) \quad (4.5)$$

The state vector  $x(k)$  includes the actual charge flow rate in (kg/s), intake oxygen concentration in (%), fuel flow rate in (kg/s) and SOI in (degree), and the input vector  $u(k)$  includes the desired state variables at time  $k$  such as

$$x(k) = \begin{bmatrix} m_c^a(k) \\ X_{o2}^a(k) \\ m_f^a(k) \\ \theta_{soi}^a(k) \end{bmatrix} \in \mathfrak{R}^4, \quad u(k) = \begin{bmatrix} m_c^d(k) \\ X_{o2}^d(k) \\ m_f^d(k) \\ \theta_{soi}^d(k) \end{bmatrix} \in \mathfrak{R}^4$$

The output vector  $y(k)$  contains the engine torque in (N-m), engine-out NOx mass flow rate in (kg/s) and specific exhaust thermal energy in (kJ/kg), and the external input vector  $d(k)$  contains the engine speed in (rad/s) and coolant temperature in (K) such as:

$$y(k) = \begin{bmatrix} T_e(k) \\ m_{nox}(k) \\ e_{exh}(k) \end{bmatrix} \in \mathfrak{R}^3, \quad d(k) = \begin{bmatrix} N_e(k) \\ T_c(k) \end{bmatrix} \in \mathfrak{R}^2$$

The system and input matrix are given by

$$A = \begin{bmatrix} 1 - \alpha_1 & 0 & 0 & 0 \\ 0 & 1 - \alpha_2 & 0 & 0 \\ 0 & 0 & 0 & 0 \\ 0 & 0 & 0 & 0 \end{bmatrix}, \quad B = \begin{bmatrix} \alpha_1 & 0 & 0 & 0 \\ 0 & \alpha_2 & 0 & 0 \\ 0 & 0 & 1 & 0 \\ 0 & 0 & 0 & 1 \end{bmatrix}$$

where  $0 < \alpha_1 < 1$  and  $0 < \alpha_2 < 1$  are the model parameters indicating limited closed-loop bandwidth of a low-level air controller due to a turbo lag and EGR gas transport delay. Note that infinite closed-loop bandwidth is assumed for low-level fuel controllers.

$h(\cdot)$  of Eqn.(4.5) is the output of polynomial regression model, described in the chapter.2 of this report. In other words, each output variable is a polynomial function of the state variables and external input variables up to the second order.

## 4.2.2 Optimal Combustion Control Design

The primary objective of this work is to develop an optimal combustion controller focused on achieving the following:

- reducing engine out NOx emissions at low load as the catalyst conversion efficiency is poor
- maximize exhaust energy for faster catalyst warm-up
- reduce fuel consumption
- meet driver torque demand while satisfying the energy management aspects mentioned above

Thus, to meet the multiple optimisation objectives, the cost function over N stages is defined as

$$J = \sum_{k=1}^N \frac{\alpha \cdot \bar{m}_{nox}(k) + \beta \cdot \bar{m}_f^a(k)}{\gamma \cdot E_{exh}(k)} \quad (4.6)$$

where  $\alpha$ ,  $\beta$  and  $\gamma$  are the positive constant weighting parameters.  $\bar{m}_{nox}(k)$  is the brake-specific engine-out NOx mass flow rate in (kg/kW-hr),  $\bar{m}_f^a(k)$  is the actual brake-specific fuel consumption in (kg/kW-hr) and  $E_{exh}(k)$  is the exhaust thermal energy rate in (kJ/s) at time  $k$ , and they are given by

$$\bar{m}_{nox}(k) = \frac{3600 \cdot m_{nox}(k)}{T_e(k) \cdot N_e(k)}$$

$$\bar{m}_f^a(k) = \frac{3600 \cdot m_f^a(k)}{T_e(k) \cdot N_e(k)}$$

$$E_{exh}(k) = e_{exh}(k) \cdot \left( m_c^a(k) + m_f^a(k) \right)$$

The proposed cost function of (4.6) meaning a budget per unit gain for catalyst light-off reflects the first three considerations. It can be lowered if the brake-specific engine-out NOx and brake-specific fuel consumption decrease while the exhaust thermal energy increases. The torque tracking requirement is implemented as a hard constraint such as

$$-0.05 \cdot T_e^d(k) \leq T_e^d(k) - T_e(k) \leq 0.05 \cdot T_e^d(k) \quad (4.7)$$

where  $T_e^d(k)$  is the torque demand by a driver. For feasible solutions, the positive constraints are added to the brake-specific engine-out NOx and exhaust thermal energy such as

$$\bar{m}_{nox}(k) \geq 0 \quad (4.8)$$

$$E_{exh}(k) \geq 0 \quad (4.9)$$

## 4.3 DP Simulation results

### 4.3.1 Sensitivity analysis

As mentioned in the section.4.1.2, the solution optimality depends on the state and control grid resolution. In this work, the engine out NOx emissions was analysed for four different grid levels of state variables, as described in the Table.4.1.

TABLE 4.1: Control factor levels and total combinations corresponding to various iterations.

Iterations	Fuel flow	Charge flow	$O_2\%$	SOI	Total combinations
Coarse	11	13	5	7	5005
Low refined	14	13	5	9	8190
High refined	21	13	5	9	12285
Final	16	13	4	7	5824

The impact of grid resolution on the optimal control problem is depicted in Fig.4.2, and it can be observed that for a given optimisation cost, as represented in Eqn.(4.6), the engine out emissions over the HD-FTP drive cycle vary significantly with state variable grid resolution.

However, it is to noted that with increase in the grid resolution though the solution optimality improves, the computation time also increases significantly, an the same is represented in Fig.4.3. In this research work, the grids were defined in a way to strike a balance between optimality and computational load. However, to further improve the optimal control performance, the grids can be further refined, but at a cost of higher computation.

For the DP framework of this work, the following state and control variable grids were considered. State grids:

- $m_f^a$  (kg/s):  $\{0.5, 1.5, \dots, 14.5, 15.5\} \times 1e^{-3}$
- $m_c^a$  (kg/s):  $\{50, 75, 100, 125, \dots, 300, 325, 350\} \times 1e^{-3}$
- $X_{o_2}^a$  (%):  $\{14, 17, 20, 23\}$
- $\theta_{soi}^a$  (deg):  $\{-10.5, -8.5, -6.5, -4.5, -2.5, -1.5, 1.5\}$

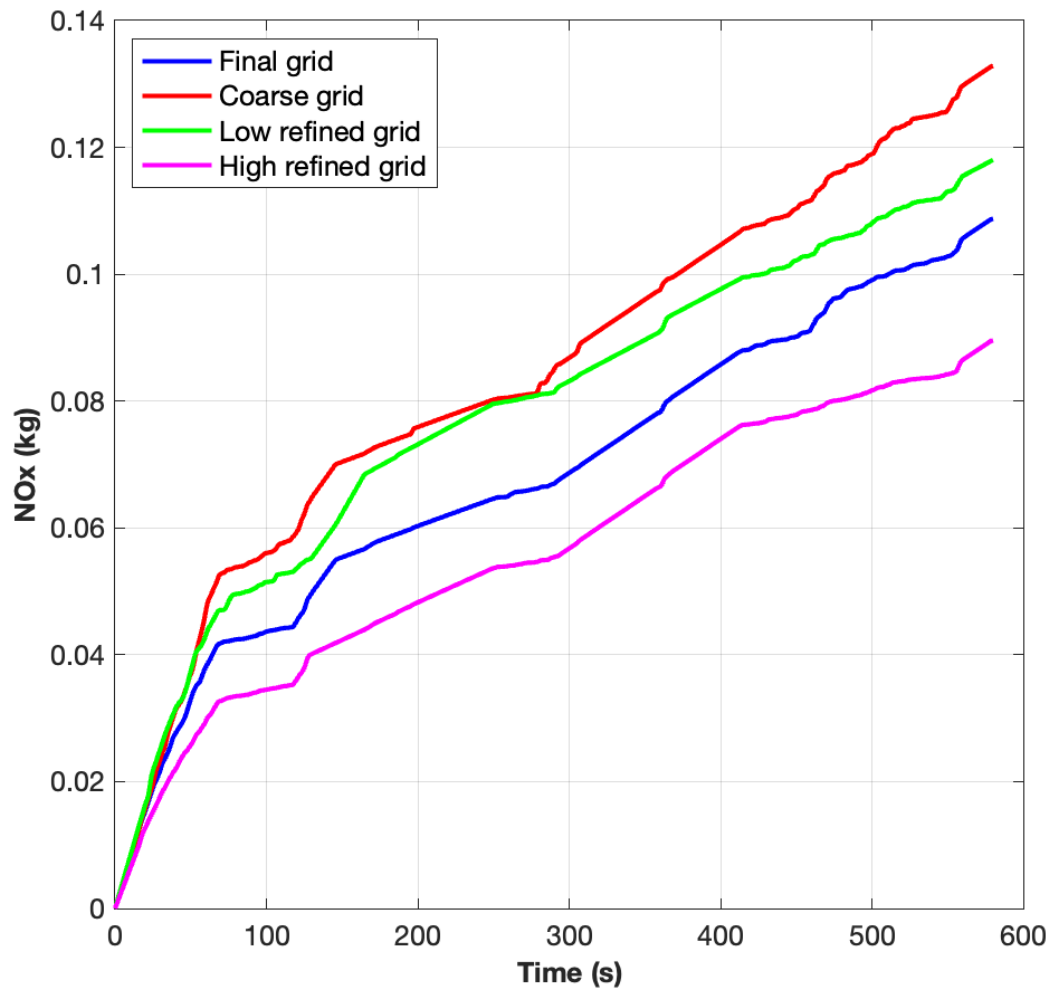


FIGURE 4.2: Engine out NOx emissions as a function of state variable grid resolution.

Control grids:

- $m_f^d$  (kg/s):  $\{0.5, 1.5, \dots, 14.5, 15.5\} \times 1e^{-3}$
- $m_c^d$  (kg/s):  $\{50, 75, 100, 125, \dots, 300, 325, 350\} \times 1e^{-3}$
- $X_{o_2}^d$  (%):  $\{14, 16, 18, 20, 22, 23\}$
- $\theta_{soi}^d$  (deg):  $\{-10.5, -8.5, -6.5, -4.5, -2.5, -1.5, 1.5\}$

### 4.3.2 Single-Objective Limit Case Studies

To understand the impact of a cost function on the optimal control commands, case studies are conducted. Each case has only one term in Eqn.(4.6). The first case is a NOx reduction only strategy as shown in Eqn.(4.10), and there is no inclusion of the fuel consumption and exhaust energy terms in the cost function. The second case is a fuel consumption reduction

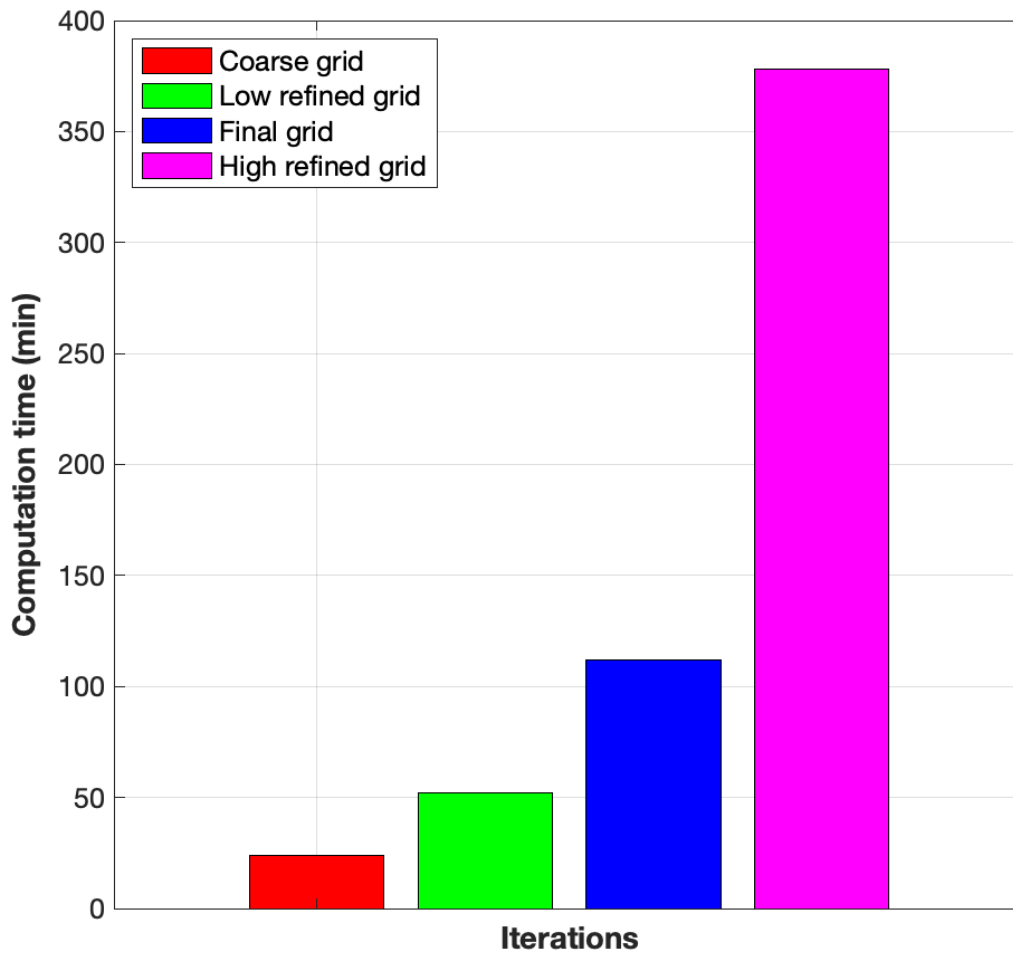


FIGURE 4.3: Computation time for various optimisation iterations.

only strategy as shown in Eqn.(4.11). The last case is a fast light-off only strategy as shown in Eqn.(4.12). Identical constraints of Eqns.(4.7), (4.8), & (4.9) apply to all cases.

$$J_{nox} = \sum_{k=1}^N \bar{m}_{nox}(k) \quad (4.10)$$

$$J_{fuel} = \sum_{k=1}^N \bar{m}_f^a(k) \quad (4.11)$$

$$J_{energy} = \sum_{k=1}^N \frac{1}{E_{exh}(k)} \quad (4.12)$$

The optimal control sequence obtained through DP simulations for the single-objective optimisation case studies is represented in Fig.4.4. For brevity, only a 10 second operation is represented.

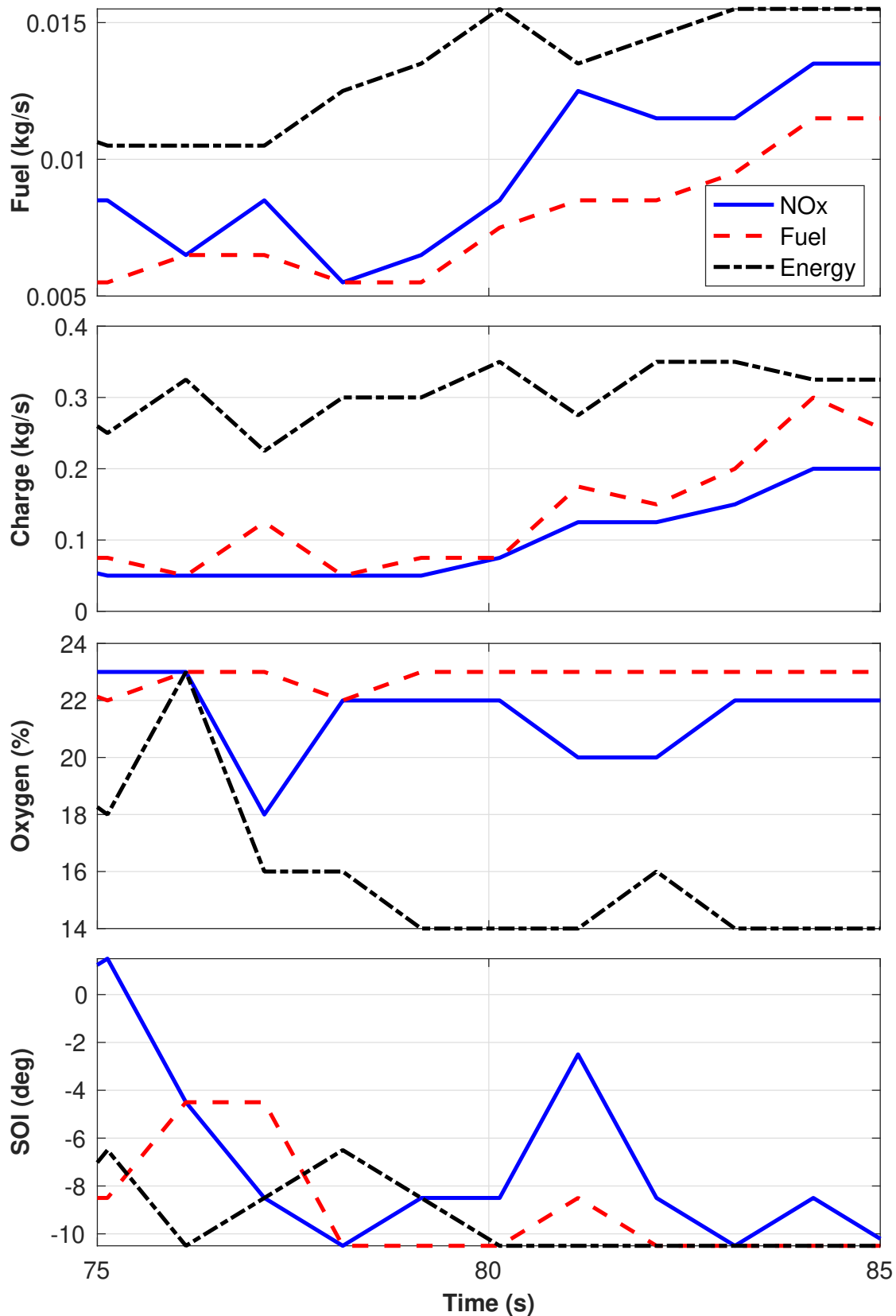


FIGURE 4.4: Optimal control sequence for different single-objective optimisation strategies.

It can be observed that for NOx optimisation strategy, the DP based controller reduces the

fresh charge availability, advances SOI and introduces EGR (reduced  $O_2$  %). Whereas, for the fast catalyst light-off, fuel flow and charge flow are increased to provide more exhaust energy (34). However, for fuel optimisation, the DP controller primarily reduces the fuel flow rate and operates the engine with no EGR. Further, the SOI is advanced to facilitate better mixing and hence efficient engine operation.

For further understanding the optimal controller sequence of different strategies, analysis on three different operational conditions shown in Table. 4.2 was carried out.

TABLE 4.2: Three operational conditions

Condition	Speed	Torque
Idle	800 (rpm)	60 (N-m)
Part load	1250 (rpm)	455 (N-m)
Full load	2400 (rpm)	750 (N-m)

From the control command comparison of different cases in Fig. 4.5, it is inferred that:

- DP controller for all operating conditions sets a rich burning environment with EGR to control NO<sub>x</sub>.
- for the fuel control strategy, the controller sets a lean operating environment and no EGR, potentially resulting in more NO<sub>x</sub> than the previous strategy.
- For a fast light-off strategy, the controller achieves high exhaust energy by increasing the exhaust gas flow rate (i.e. charge flow rate + fuel flow rate), but introduces a large amount of EGR gas to prevent torque shoot-up, thus ensuring torque tracking.

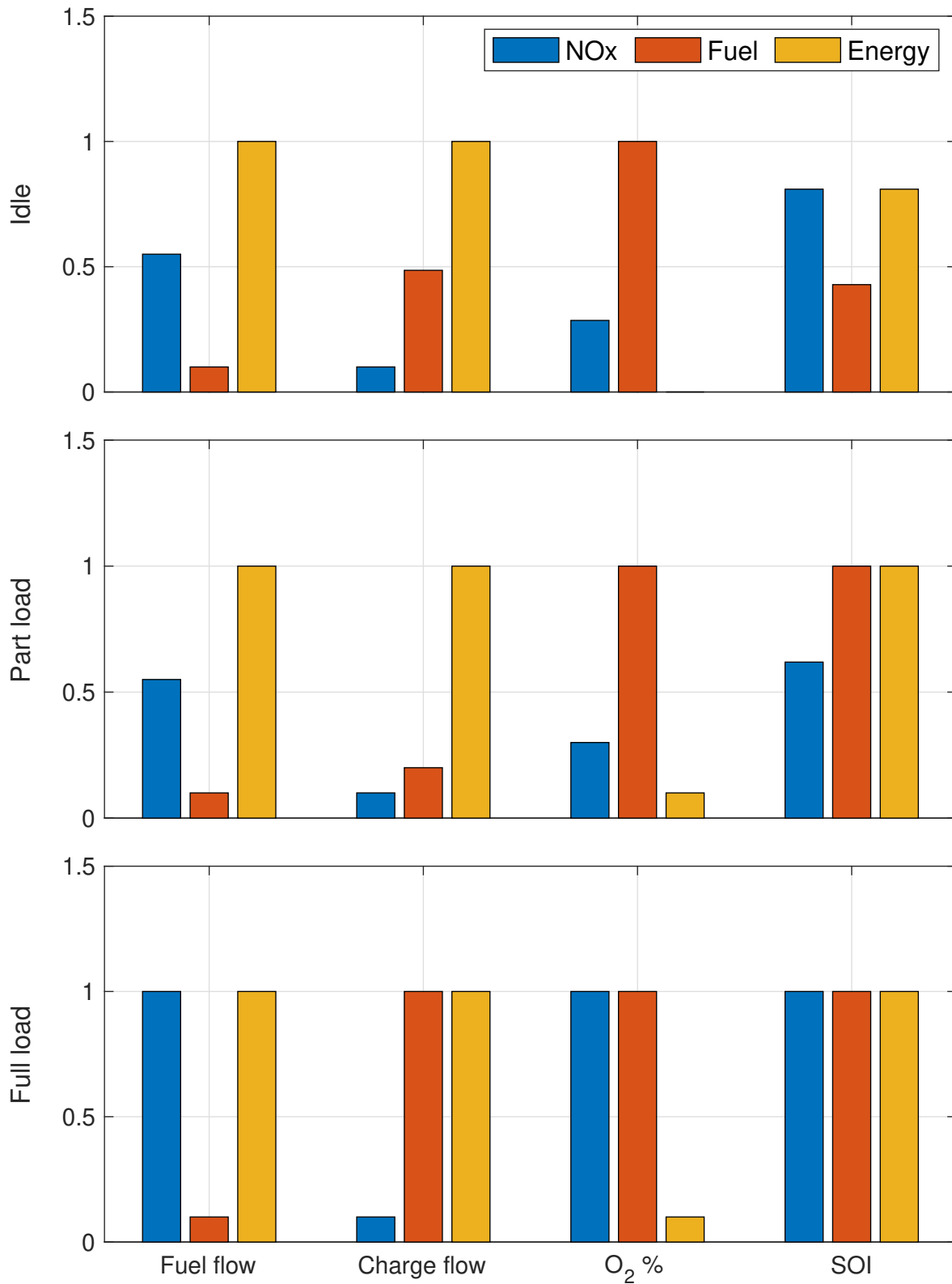


FIGURE 4.5: Normalized optimal control sequence for three different strategies during idle, part load and full load conditions. Note that positive SOI means before-top-dead-center in this figure.

### 4.3.3 Multi-Objective Optimization

In this section, the performance of the multi-objective cost function represented in Eqn.(4.6) is discussed. Three different case studies were conducted, each with a different set of cost weights, as described in Table.4.3. A higher weight signifies optimization priority, and the DP optimal controller adopts a high-level control sequence accordingly.

TABLE 4.3: Weighting parameters

Iterations	$\alpha$	$\beta$	$\gamma$
ITR 1	0.6	0.2	0.2
ITR 2	0.2	0.6	0.2
ITR 3	0.2	0.2	0.6

The system performance of different iterations over the HD FTP drive cycle are shown in Fig.4.6. The three thin curves are for the limit cases, respectively. And the three bold curves are for the different weights shown in Table.4.3. The trade-off between NOx emissions, exhaust energy for light-off and fuel consumption is evident from the limit cases. It was observed that after 200 seconds into the drive cycle:

- the exhaust energy for ITR 1 is 12 % higher than the single objective NOx control case, thus confirming the potential for faster catalyst light-off.
- ITR 1 results in lowest NOx emissions among the three multi-objective iterations.
- The fuel consumption is about 5 % higher compared to the single objective NOx control case.

Thus, with NOx control and fast catalyst light-off as the primary objectives of this work, ITR 1 turns out to yield the best multi-objective optimisation performance.

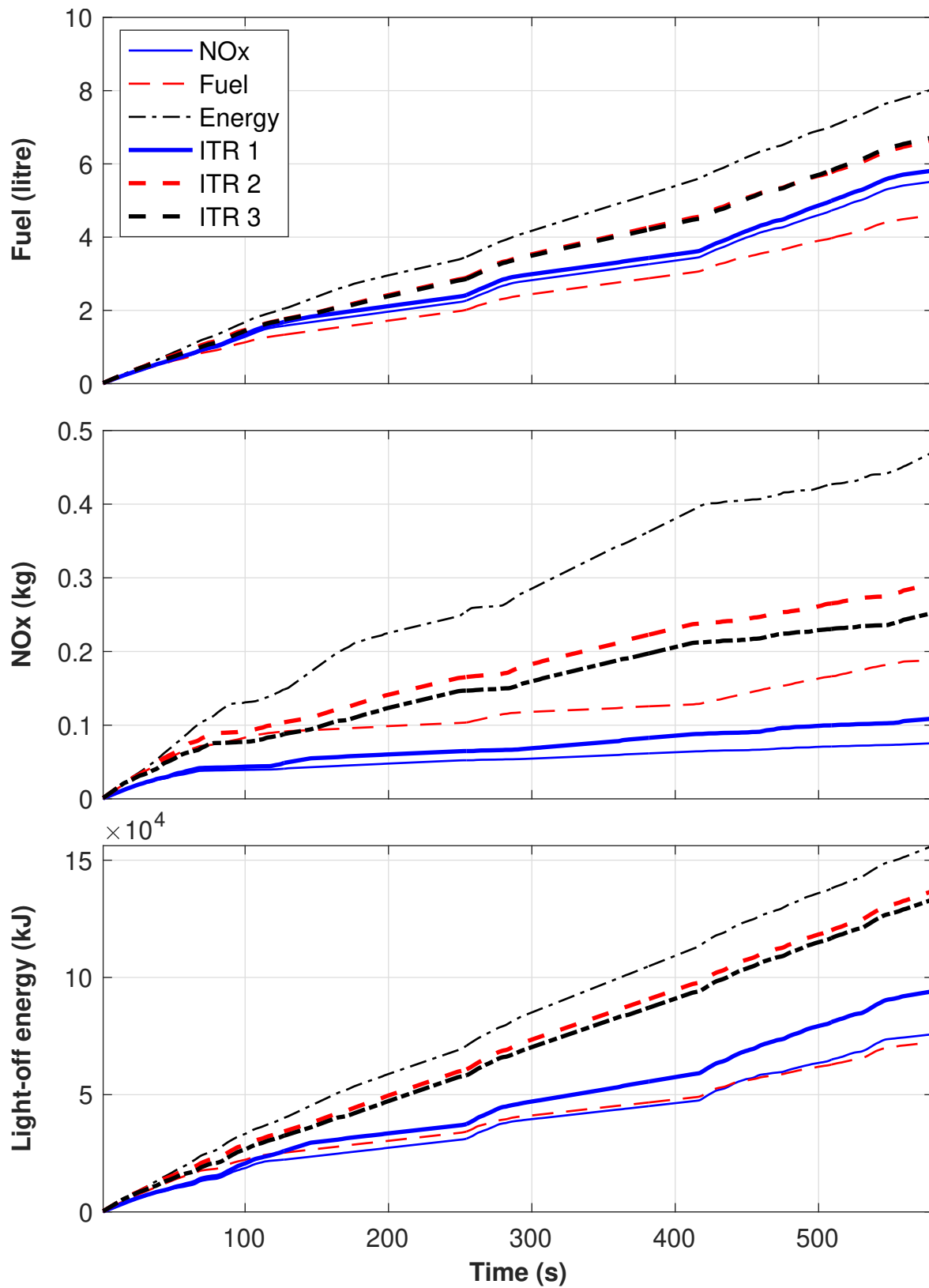


FIGURE 4.6: Performance comparison among different strategies.

## Chapter 5

# Scope for future work

The major work carried out in this thesis focused on developing a control-oriented combustion model and later obtaining a globally optimal control sequence of engine parameters for a multi-objective optimisation problem. However, the method adopted for a globally optimal solution using DP requires prior information on the drive cycle, which is seldom available in real word operation. Thus, there is a need to develop a real-time implementable controller that can be deployed in a vehicle through calibration to achieving the desired reductions in emissions and fuel consumption.

In this research work, a preliminary study on the possibility of adopting a reinforcement-learning (*RL*) based combustion controller was performed. However, because of constraints in the developmental timelines of the thesis, the work could not be finished. The *RL* framework considered for a real-time implementable combustion controller is described briefly in this chapter, and the reader may refer to the framework for future work.

### 5.1 Reinforcement Learning Background

RL is a branch of machine learning alongside supervised and unsupervised learning. RL is a computational approach to understanding and automating goal-directed learning and decision-making. RL distinguishes itself from other machine learning approaches by learning from the direct interaction of an agent with its environment without relying on exemplary supervision [28].

#### 5.1.1 Elements of Reinforcement Learning

A typical RL problem comprises the following elements:

- agent
- environment
- reward signal
- policy
- value function.

For an in depth understanding about the types of RL agents and the other elements, the reader is advised to refer to the subsequent sections in [28].

### 5.1.2 RL framework

In an RL-based controller, the agent performs the control actions, and the subsequent changes in the environment (system response) corresponding to each action are stored. Each desirable action sequence is rewarded with a positive incentive, defined based on the goal of the control problem at hand, and the undesirable actions are penalised. The system learns based on the reward signal through agent-environment interactions, as depicted in Fig.5.1 [28], and the optimal control sequence (policy) is the one that maximises the reward.

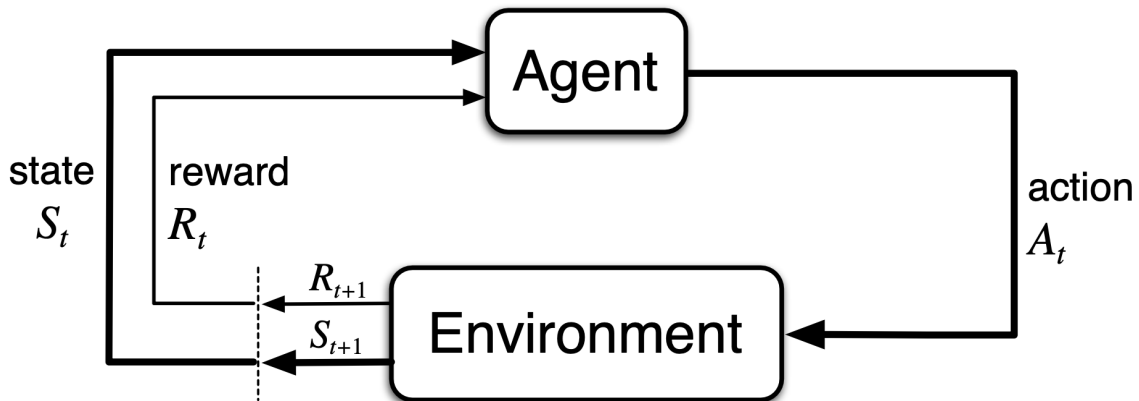


FIGURE 5.1: The agent-environment interaction in an RL framework.

## 5.2 RL based combustion controller

This section focuses on an overview of the integration of the control-oriented HD diesel engine model within the RL framework. For developing this work, a Deep Deterministic Policy Gradient (*DDPG*) RL agent was selected because of its ability to work with continuous signals.

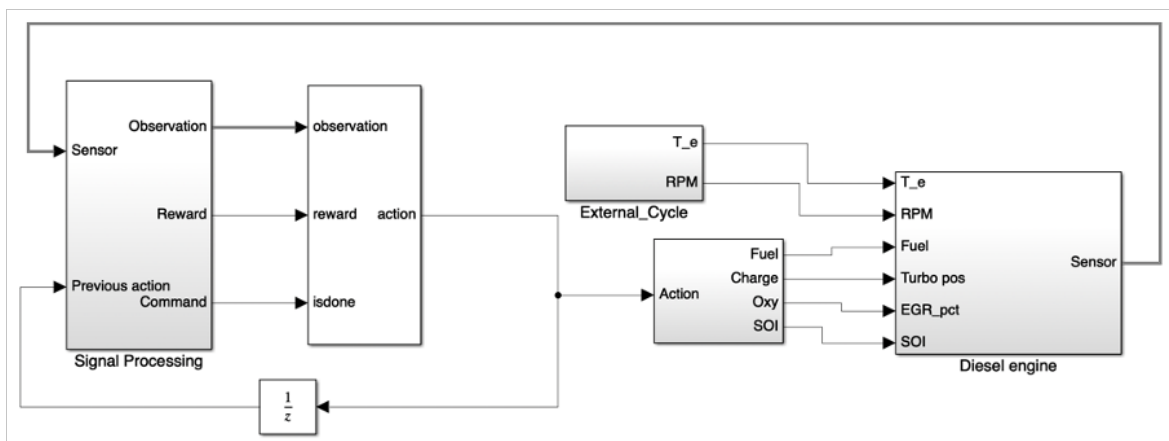


FIGURE 5.2: Simulink block diagram of HD Diesel engine model within RL framework.

### 5.2.1 RL environment

The RL control-oriented HD diesel engine model was defined as an environment. The environment takes  $m_f, m_c, O_2\%, SOI$  commands from the RL agent, along with external drive cycle commands of  $N_e$  and  $T_c$  as inputs, and generates  $T_e, (m_{NOx})$  and  $E$  as states (system responses).

### 5.2.2 Reward function

The reward for the RL framework in this thesis work consists of three terms, one each for torque tracking, multi objective optimization term & control actions, where high control actions are penalized.

- If  $T_e, m_{NOx}, E < 0$  or  $|T_{err}| > 5\%$ , then a negative reward of -0.5 (per time step) is assigned.
- While  $T_{err} < 5\%$ , the reward is assigned based on torque tracking accuracy as  $e^{(5-|T_{err}|)}$ .
- The reward for emission optimization is calculated as  $\frac{\gamma \cdot E_{exh}}{\alpha \cdot \bar{m}_{nox} + \beta \cdot \bar{m}_f^a}$ , where  $\alpha, \beta, \gamma$  are the weights corresponding to optimal strategy ITR 1 in Chapter.4.

### 5.2.3 Actions

Based on the control policy of the RL framework, the *DDPG* RL agent in this thesis work will set  $m_f, m_c, O_2\%, SOI$  as actions on the environment. The dynamic time responses of these actions are then considered as inputs for the control-oriented model of the HD diesel engine (environment).

## 5.3 Summary

Due to constraints in the development timeline of this thesis work, this section on an RL-based real-time implementable controller focuses only on the framework and the reward function adopted in this thesis work.

Thus, the reader is advised to refer the aspects of RL for an in-depth understanding of RL parameters and hyperparameters. However, the implementation of a control-oriented model within an RL framework and designing its reward function can still be referred from this work.



## Chapter 6

# Conclusion

With the rising concern of climate change, the global automotive industry is witnessing a paradigm shift towards cleaner mobility. The ultra-low nitrogen oxides (NO<sub>x</sub>) regulation, proposed by the California Air Resource Board, will require a 90 % reduction in tailpipe NO<sub>x</sub> emission from the current standards implemented in 2010 without increasing greenhouse gas emissions. For compliance with this stringent regulation, it is essential to achieve low engine-out NO<sub>x</sub> and fast catalyst light-off simultaneously during cold start and low-load conditions.

This thesis work presents a model-based optimal high-level combustion controller for HD diesel engines for achieving the multi-objective optimal control problem of emission control and faster catalyst light-off. The work establishes a way of obtaining control-oriented combustion models using Neural networks and polynomial modelling.

The research then focuses on developing a Dynamic Programming-based high-level optimal combustion controller to find globally optimal solutions for the desired fuel flow rate, charge flow rate, intake oxygen percentage, and SOI for a given drive cycle. The high-level optimal control sequences are then achieved by low-level air and fuel controllers, which is beyond the scope of this work. The multi-objective cost function for optimisation is defined such that the weighting parameters can be flexibly calibrated. Numerical studies carried out in this work demonstrate that the proposed method can deal with conflicting requirements in an effective way. This method also has the potential to give insight into calibrations of diesel engine control maps.

Later, the possibility of an online implementable Reinforcement-learning based real-time combustion controller was studied as a part of this thesis work. However, the work could not be completed due to the timeline and administrative issues. However, the reinforcement learning-based online combustion controller can be explored in future studies.



# Bibliography

1. Heywood JB. Internal combustion engine fundamentals. McGraw-Hill Education, 2018
2. Alkidas A. The influence of partial suppression of heat rejection on the performance and emissions of a divided-chamber diesel engine. *SAE transactions* 1986 :349–59
3. Lloyd AC and Cackette TA. Diesel Engines: Environmental Impact and Control. *Journal of the Air & Waste Management Association* 2001; 51:809–47
4. Pradyumna S. Automotive diesel tradeoff. 2020
5. Sharp C, Neely G, Zavala B, and Rao S. CARB Low NOX Stage 3 Program-Final Results and Summary. *SAE International Journal of Advances and Current Practices in Mobility* 2021; 3:1508–25
6. Kumar A, Ingram K, Goyal D, and Kamasamudram K. Impact of Carbonaceous Compounds Present in Real-World Diesel Exhaust on NOx Conversion over Vanadia-SCR Catalyst. *SAE International Journal of Engines* 2016; 9:1598–603
7. Schijndel J van, Donkers M, Willems F, and Heemels W. Dynamic programming for integrated emission management in diesel engines. *IFAC World Congress*. Cape Town, South Africa. Elsevier, 2014 :11860–5
8. Borek J, Groelke B, Earnhardt C, and Vermillion C. Economic optimal control for minimizing fuel consumption of heavy-duty trucks in a highway environment. *IEEE Trans. Control Systems Technology* 2019; 28:1652–64
9. Mathworks. CI Engine Project Template. <https://www.mathworks.com/help/autoblks/ug/ci-engine-project-template.html>. 2021
10. McKay MD, Beckman RJ, and Conover WJ. A comparison of three methods for selecting values of input variables in the analysis of output from a computer code. *Technometrics* 2000; 42:55–61
11. Federic G. LHS DOE generator. <https://www.mathworks.com/matlabcentral/fileexchange/57657-lhs-doe-generator> , MATLABCentralFileExchange. 2021
12. d’Ambrosio S, Finesso R, Fu L, Mittica A, and Spessa E. A control-oriented real-time semi-empirical model for the prediction of NOx emissions in diesel engines. *Applied Energy* 2014; 130:265–79
13. Gärtner U, Hohenberg G, Daudel H, and Oelschlegel H. Development and application of a semi-empirical NO x model to various HD diesel engines. *Thermo-and Fluid Dynamic Processes in Diesel Engines 2*. Springer, 2004 :285–312
14. Krishnan A, Sekar VC, Balaji J, and Boopathi S. Prediction of NOx reduction with exhaust gas recirculation using the flame temperature correlation technique. *Proceedings of the National Conference on Advances in Mechanical Engineering*. 2006 :18–9
15. Guardiola C, López J, Martín J, and García-Sarmiento D. Semiempirical in-cylinder pressure based model for NOx prediction oriented to control applications. *Applied Thermal Engineering* 2011; 31:3275–86

16. Arrègle J, López JJ, Guardiola C, and Monin C. Sensitivity study of a NO<sub>x</sub> estimation model for on-board applications. Tech. rep. SAE Technical Paper, 2008
17. De Cesare M and Covassin F. Neural Network Based Models for Virtual NO<sub>x</sub> Sensing of Compression Ignition Engines. Tech. rep. SAE Technical Paper, 2011
18. Rojas R. Neural networks: a systematic introduction. Springer Science & Business Media, 2013
19. Kollmannsberger S, D'Angella D, Jokeit M, Herrmann L, et al. Deep Learning in Computational Mechanics. Springer, 2021
20. Finesso R, Spessa E, Yang Y, Conte G, and Merlino G. Neural-network based approach for real-time control of BMEP and MFB50 in a Euro 6 diesel engine. *SAE Technical Paper*. 2017-24-0068. 2017
21. Lew A and Mauch H. Dynamic programming: A computational tool. Vol. 38. Springer, 2006
22. Bertsekas D. Dynamic programming and optimal control: Volume I. Vol. 1. Athena scientific, 2012
23. Millo F, Rolando L, and Servetto E. Development of a control strategy for complex light-duty diesel-hybrid powertrains. Tech. rep. SAE Technical Paper, 2011
24. Johri R and Filipi Z. Optimal energy management of a series hybrid vehicle with combined fuel economy and low-emission objectives. *Proceedings of the Institution of Mechanical Engineers, Part D: Journal of Automobile Engineering* 2014; 228:1424–39
25. Serrao L, Onori S, and Rizzoni G. A comparative analysis of energy management strategies for hybrid electric vehicles. 2011
26. Miretti F, Misul D, and Spessa E. DynaProg: Deterministic Dynamic Programming Solver for Finite Horizon Multi-stage Decision Problems. *SoftwareX* 2021; 14:100690
27. Sundstrom O and Guzzella L. A generic dynamic programming Matlab function. 2009 *IEEE control applications,(CCA) & intelligent control,(ISIC)*. IEEE. 2009 :1625–30
28. Sutton RS and Barto AG. Reinforcement learning: An introduction. MIT press, 2018